

Authors are encouraged to submit new papers to INFORMS journals by means of a style file template, which includes the journal title. However, use of a template does not certify that the paper has been accepted for publication in the named journal. INFORMS journal templates are for the exclusive purpose of submitting to an INFORMS journal and should not be used to distribute the papers in print or online or to submit the papers to another publication.

Fabrication-Adaptive Optimization, with an Application to Photonic Crystal Design

Han Men

Department of Aeronautics & Astronautics, Massachusetts Institute of Technology, Cambridge, MA 02139, abbymen@mit.edu

Robert M. Freund

Sloan School of Management, Massachusetts Institute of Technology, Cambridge, MA 02139, rfreund@mit.edu

Ngoc C. Nguyen, Joel Saa-Seoane, Jaime Peraire

Department of Aeronautics & Astronautics, Massachusetts Institute of Technology, Cambridge, MA 02139, cuongng@mit.edu, jsaa@mit.edu, peraire@mit.edu

It is often the case that the computed optimal solution of an optimization problem cannot be implemented directly, irrespective of data accuracy, due to either (i) technological limitations (such as physical tolerances of machines or processes), (ii) the deliberate simplification of a model to keep it tractable (by ignoring certain types of constraints that pose computational difficulties), and/or (iii) human factors (getting people to “do” the optimal solution). Motivated by this observation, we present a modeling paradigm called “fabrication-adaptive optimization” for treating issues of implementation/fabrication. We develop computationally-focused theory and algorithms, and we present computational results for incorporating considerations of implementation/fabrication into constrained optimization problems that arise in photonic crystal design. The fabrication-adaptive optimization framework stems from the robust regularization of a function. When the feasible region is not a normed space (as typically encountered in application settings), the fabrication-adaptive optimization framework typically yields a non-convex optimization problem. (In the special case where the feasible region is a finite-dimensional normed space, we show that fabrication-adaptive optimization can be re-cast as an instance of modern robust optimization.) We study a variety of problems with special structures on functions, feasible regions, and norms, for which computation is tractable, and develop an algorithmic scheme for solving these problems in spite of the challenges of non-convexity. We apply our methodology to compute fabrication-adaptive designs of two-dimensional photonic crystals with a variety of prescribed features.

Key words: fabrication adaptivity, robust regularization, bandgap optimization, photonic crystal design

1. Introduction: Problem Statement, Preliminaries, and Computational Aspirations

Consider a general constrained optimization problem of the form:

$$\begin{aligned} z^* = \min_x & f(x) \\ \text{s.t. } & x \in S, \end{aligned} \tag{1}$$

where $S \subseteq \mathbb{R}^n$ is the feasible region, and $f(\cdot) : \mathbb{R}^n \rightarrow \mathbb{R}$ is the objective to be optimized. The context of (1) may be as diverse as portfolio optimization (Best 2010) where x_i is the number of shares to be invested in asset i , to optimal microstructure material design where x_i is the concentration of

a dielectric material in pixel (or voxel) i of a discretized physical region as in Men et al. (2010, 2011). Let x^* be an optimal solution of (1). The notion of *fabrication-adaptivity*, or perhaps more generally *implementation-adaptivity*, has to do with the concern that while the data and other descriptors of the problem may be quite accurate, it may be generically implausible to implement the optimal solution x^* exactly. Some reasons for this may include:

1. Technological limitations. For example, the production or fabrication technology might not be able to fabricate the product exactly according to the plan specified in x^* , perhaps due to limitations of machine tolerances,
2. Deliberate simplifications. The model (1) may be a deliberate simplification of the real problem in order for the optimization model to be computationally tractable. For example, it may be computationally prohibitive to include odd-lot constraints in a portfolio optimization model, or connectivity constraints in a microstructure material design model, etc., or
3. Human factors. It may be implausible to assume that people will “do” x^* precisely as the optimization model prescribes.

Indeed, the application that has given rise to this line of study is a nonlinear optimization problem arising in microstructure material design (Men et al. 2010), where $S := [x_{\min}, x_{\max}]^n = \{x \in \mathbb{R}^n : x_{\min}e \leq x \leq x_{\max}e\}$ is a hypercube with $n \gg 0$, and the component values x_i represent the permittivity of a dielectric material at pixel (or voxel) i for $i = 1, \dots, n$. The values x_{\min} and x_{\max} correspond to permittivity constants for air and the dielectric material (e.g., gallium arsenide), respectively. The objective is to determine a design for which a prescribed relative eigenvalue bandgap ($2 \frac{\lambda_{m+1} - \lambda_m}{\lambda_{m+1} + \lambda_m}$) is maximized, where λ_m is the m^{th} eigenvalue of a certain system. The resulting optimization problem is nonlinear, non-convex, and large-scale; nevertheless effective methods for computing solutions are developed in Men et al. (2010, 2011). (In fact, a more proper microstructure material design model should use binary conditions $x_i \in \{x_{\min}, x_{\max}\}$ instead of the interval restrictions $x_i \in [x_{\min}, x_{\max}]$; such binary conditions are typically relaxed in the bandgap optimization problems with almost no degradation in solution quality, see Men et al. (2010).) The computed solution x^* might not be fabricable due to small feature sizes (disconnected pixels with $x_i = x_{\max}$) or complicated material interfaces (such as roughness of boundaries). In principle one can add constraints to ensure that features are not small and/or ensure smooth boundaries of surfaces of the material, but such an approach is decidedly unattractive as it leads to an exponential number of constraints – and makes a complex model even more complex computationally. Instead we proceed as follows. First we observe that it is relatively easy in practice to use human judgment to modify a given design solution x to a fabricable solution y by switching the concentration of material at a relatively small number δ of pixels from x_{\min} to x_{\max} (or *vice versa*) to remove small features and/or rough material interfaces, and hopefully not degrade the objective function value too much in the process. Here we presume that $\delta \ll n$. If we anticipate that we will need to perform some sort of manual modification of a solution x , then it is beneficial to account for this *a priori* in the model specification. This is the basic idea of *fabrication-adaptive optimization* which we now formally describe.

For a generic optimization problem of the form (1), let x be a feasible and/or optimal solution. The basic premise of our approach is that we will fabricate/implement some solution y that is close to x in some prescribed norm, say at most a distance δ from x in the prescribed norm, and that such a nearby fabricable solution y is very easy to determine/compute for any given solution x . We construct the FA (for *fabrication-adaptive*) counterpart objective function $\tilde{f}(\cdot)$ of the original objective function $f(\cdot)$ in (1), as follows:

$$\begin{aligned} \tilde{f}(x) := \max_y \quad & f(y) \\ \text{s.t.} \quad & \|y - x\| \leq \delta \\ & y \in S, \end{aligned} \tag{2}$$

where $\delta > 0$ is the fabrication-adaptive (FA) parameter, and $\|\cdot\|$ is the prescribed norm. Then $\tilde{f}(x)$ is a (conservative) upper bound on the objective function value of any (fabricable) solution y whose distance from x is at most δ in the prescribed norm. We then construct the fabrication-adaptive optimization problem which is defined as:

$$\begin{aligned} \tilde{z}^* = \min_x \quad & \tilde{f}(x) \\ \text{s.t.} \quad & x \in S. \end{aligned} \quad (3)$$

The FA optimization problem (3) seeks to optimize the conservative FA counterpart $\tilde{f}(\cdot)$ of the original objective function $f(\cdot)$. In this way the FA model seeks to produce a solution x_{FA}^* which is more adaptable to modification to a nearby fabricable solution y whose objective value $f(y)$ is not significantly degraded.

The functional form (2) was first introduced by Lewis (2002) for the special case when S is a finite-dimensional normed space (essentially $S = \mathbb{R}^n$ without loss of generality) and with the norm $\|\cdot\|$ replaced by a more general gauge function $g(\cdot)$ (Rockafellar 1970), where it was called the “robust regularization” of $f(\cdot)$. The term “robust regularization” is appropriate for the context given therein, which includes issues of uncertain data in the construction of $f(\cdot)$, uncertain implementation issues, and the like. Indeed, the function $f(\cdot)$ in Lewis (2002) is considered broadly and so might be a constraint function or an objective function in an optimization problem, or perhaps simply a function of interest. The name “robust regularization” is also suggestive of a relationship to robust optimization (Ben-Tal et al. 2009, Bertsimas et al. 2011), and it turns out that in the very special case when $S = \mathbb{R}^n$, the model (2)-(3) can be formatted as a particular instance of a robust optimization problem; this is shown herein in Appendix A. However, when $S \neq \mathbb{R}^n$ (as one would typically expect), the connection between (2)-(3) and robust optimization breaks down; this is also shown in Appendix A. Lewis and Pang (2009) generalizes the definition of the robust regularization to the case when $S \neq \mathbb{R}^n$, and presents a variety of results regarding smoothness of $\tilde{f}(\cdot)$ and related mathematical properties. In somewhat of a contrast, the focus of this paper is on the model (2)-(3) as a mechanism for fabrication-adaptive optimization; as such we rely on the premise articulated above that we will fabricate/implement some solution y that is close to x in some prescribed norm, say at most a distance δ from x in the prescribed norm, and that such a nearby fabricable solution y is very easy to determine/compute for any given solution x . For this setting we expect $S \neq \mathbb{R}^n$, whereby there is no connection to robust optimization. In the context of our intended modeling set-up, the premise of adapting the solution after-the-fact to a nearby fabricable solution, and the fact that typically $S \neq \mathbb{R}^n$, we prefer to use the term “fabrication-adaptive optimization” rather than “robust regularization” for the paradigm (2)-(3) as it is more aligned with aspirations of modeling, application, optimization, and computation.

The notion of fabrication adaptivity is also related to the modeling of implementation errors. Luo (2003) and Luo et al. (2004) consider such models in the context of signal processing and digital communication, where solutions are affected by errors due to discretization of the signal. Pinar and Arıkan (2004) examines modeling of implementation errors in linear least-squares problems (of which signal processing is an application), and Stinstra and Den Hertog (2008) considers implementation errors in generic optimization modeling through the lens of various types of modeling errors. The implementation-error models developed in these works implicitly assume that the set of possible errors is independent of the solution point, therefore in this case, the modeling of implementation errors can be treated as an instance of robust optimization (Ben-Tal et al. 2009, Bertsimas et al. 2011). This contrasts with fabrication adaptive optimization, as is discussed in Appendix A.

1.1. Basic Non-Convexity Issues, and Practical and Computational Aspirations

In a realistic application of the fabrication-adaptive model (2)-(3) one would typically have $S \neq \mathbb{R}^n$. However, at least from an academic perspective, the special case of $S = \mathbb{R}^n$ gives rise to interesting properties with respect to convexity and with respect to connection to the modern domain of *robust optimization*, see Ben-Tal et al. (2009) and Bertsimas et al. (2011). When $S = \mathbb{R}^n$, the fabrication-adaptive objective function $\tilde{f}(\cdot)$ is convex if $f(\cdot)$ is convex, see Proposition 3.1 of Lewis (2002). Again when $S = \mathbb{R}^n$, it is also straightforward to show that quasiconvexity is preserved as well: if $f(\cdot)$ is quasiconvex, then the fabrication-adaptive objective function $\tilde{f}(\cdot)$ is quasiconvex.

When $S \neq \mathbb{R}^n$, the following example shows that the FA counterpart optimization problem of a convex optimization problem need not be convex.

EXAMPLE 1. (A non-convex FA objective function when $f(\cdot)$ is convex.) Let $S = \{x \in \mathbb{R}^2 : 0 \leq x \leq e\}$, the unit 2-dimensional square, and consider the convex (linear) objective function $f(x) := 2x_1 + x_2$, and let $\|\cdot\| = \|\cdot\|_1$ and $\delta = 1/10$ for concreteness. At $x^1 := (1 - 2\delta, 1)$ we have

$$\tilde{f}(x^1) = \max\{2y_1 + y_2 : 0 \leq y \leq e, \|y - x^1\|_1 \leq \delta\} = 3 - 2\delta.$$

At $x^2 := (1, 1 - 3\delta)$ we have

$$\tilde{f}(x^2) = \max\{2y_1 + y_2 : 0 \leq y \leq e, \|y - x^2\|_1 \leq \delta\} = 3 - 2\delta.$$

However, at $x^3 := \frac{1}{2}x^1 + \frac{1}{2}x^2 = (1 - \delta, 1 - 3\delta/2)$ we have:

$$\tilde{f}(x^3) = \max\{2y_1 + y_2 : 0 \leq y \leq e, \|y - x^3\|_1 \leq \delta\} = 3 - 3\delta/2.$$

In this case we have $\tilde{f}(x^3) = 3 - 3\delta/2 > 3 - 2\delta = \max\{\tilde{f}(x^1), \tilde{f}(x^2)\}$, thus showing that $\tilde{f}(\cdot)$ is not even quasiconvex on the feasible region S , as the level set $L_\beta := \{x \in S : \tilde{f}(x) \leq \beta\}$ is not convex for $\beta = 3 - 2\delta$.

In light of the fact that the FA optimization problem (2)-(3) can be non-convex, it makes most practical sense to consider using the FA modeling paradigm when the original function $f(\cdot)$ in (1) is not convex. (Otherwise we are doing the computational unpromising task of transforming a nominally convex problem into a non-convex problem.) We therefore will take as given that $f(\cdot)$ is not required to be convex, and that we expect the FA optimization problem (2)-(3) to be non-convex. In consideration of goals of algorithms, we aspire to compute solutions \bar{x} of (2)-(3) that are either local optima or perhaps just have “good” objective function value $\tilde{f}(\bar{x})$ where such “goodness” will of necessity be problem/context-dependent. In order to design algorithms to solve the FA optimization problem (2)-(3), we focus on two computational tasks that seem natural to require in order to design useful algorithms: (i) computing the FA counterpart function value $\tilde{f}(x)$ for a given $x \in S$, and (ii) computing first-order function objects such as the gradient $\nabla \tilde{f}(x)$ or a (perhaps only local) subgradient of $\tilde{f}(x)$ or of the “pieces” of $\tilde{f}(\cdot)$ in the case when $\tilde{f}(\cdot)$ is the pointwise maximum of other functions, for a given $x \in S$. For a given $x \in S$, notice from (2) that computing $\tilde{f}(x)$ is itself generally intractable as it involves maximizing a convex function over a convex set. Nevertheless, in many useful instances with special structure on $f(\cdot)$, S , and/or $\|\cdot\|$, it will be computationally tractable to compute $\tilde{f}(\cdot)$ and $\nabla \tilde{f}(\cdot)$ (or other first-order information) efficiently. Indeed, one of the main concerns of the rest of this paper is with special structures of real interest for which computation with the FA counterpart function $\tilde{f}(\cdot)$ is relatively efficient (Section 2), and with the practical use of the FA paradigm for solving problems that gave rise to this paradigm in the first place, namely bandgap optimization problems (Sections 3 and 4). In Section 2 we examine FA optimization problems with certain structures of interest, mainly functions that are in turn piecewise-linear, linear fractional, piecewise linear fractional, as well as a canonical eigenvalue function. We also propose an algorithm for FA optimization in the piecewise linear

fractional case. In Section 3, we review the class of design optimization problems known as band-gap problems that arise in engineering design optimization, and we show how the FA optimization paradigm can be applied to these problems. In Section 4 we present computational results from applying the FA optimization to various bandgap problems that arise in photonic crystal design, and we demonstrate that our proposed algorithm succeeds in producing much improved adaptive and fabricable solutions.

1.2. Notation

Let $e = (1, \dots, 1)$ denote the vector of ones, whose dimension will be given in context. Let $\|\cdot\|$ denote a norm on \mathbb{R}^n , and let $\|\cdot\|_*$ be the associated dual norm, namely $\|v\|_* := \max\{v^T x : \|x\| \leq 1\}$. The ball of radius δ centered at \bar{x} is denoted $B(\bar{x}, \delta) := \{x : \|x - \bar{x}\| \leq \delta\}$. Recall that a function $f(\cdot)$ on S is convex if $f(\alpha x + (1 - \alpha)y) \leq \alpha f(x) + (1 - \alpha)f(y)$ for any $\alpha \in [0, 1]$ and all $x, y \in S$. Similarly, $f(\cdot)$ on S is quasiconvex if $f(\alpha x + (1 - \alpha)y) \leq \max\{f(x), f(y)\}$ for any $\alpha \in [0, 1]$ and all $x, y \in S$, and $f(\cdot)$ is concave or quasiconcave if $-f(\cdot)$ is convex or quasiconvex, respectively. Note that $f(\cdot)$ is quasiconvex if and only if the lower level sets of $f(\cdot)$ are convex sets, see Avriel (1976). If $f(\cdot)$ is convex on S , then $g \in \mathbb{R}^n$ is a subgradient of $f(\cdot)$ at $\hat{x} \in S$ if $f(x) \geq f(\hat{x}) + g^T(x - \hat{x})$ for all $x \in S$. Similarly for a concave function on S , $g \in \mathbb{R}^n$ is a subgradient of $f(\cdot)$ at $\hat{x} \in S$ if $f(x) \leq f(\hat{x}) + g^T(x - \hat{x})$ for all $x \in S$. A function $f(\cdot)$ on S is locally convex at $\hat{x} \in S$ if there exists some $\delta > 0$ for which $f(\cdot)$ is convex on $S \cap B(\hat{x}, \delta)$, and we say that g is a local subgradient of $f(\cdot)$ at \hat{x} if $f(x) \geq f(\hat{x}) + g^T(x - \hat{x})$ for all $x \in S \cap B(\hat{x}, \delta)$. Similar remarks hold for local concavity and a local subgradient of a locally concave function. Let X, Y be any symmetric matrices. We write “ $X \succeq 0$ ” to denote that X is symmetric and positive semidefinite, “ $X \succeq Y$ ” to denote that $X - Y \succeq 0$, and “ $X \succ 0$ ” to denote that X is positive definite. If $K \subset \mathbb{R}^n$ is a closed convex cone, then its dual cone K^* is defined by $K^* := \{s \in \mathbb{R}^n : s^T x \geq 0 \text{ for all } x \in K\}$.

2. Fabrication-Adaptive Optimization Problems with Special Structures

We study some FA optimization problems with special structures on $f(\cdot)$, S , and/or $\|\cdot\|$.

2.1. Three Special Structures for $S = \mathbb{R}^n$

We show three classes of examples of special structures for instances where $S = \mathbb{R}^n$. In the first class the objective function is the maximum of a finite number of affine functions:

$$f(x) := \max_{i=1, \dots, m} b_i + (a^i)^T x, \quad (4)$$

and $S = \mathbb{R}^n$. It is easy to derive the fabrication-adaptive objective function in this case:

$$\begin{aligned} \tilde{f}(x) &= \max_{\|y-x\| \leq \delta} \max_{i=1, \dots, m} b_i + (a^i)^T y \\ &= \max_{i=1, \dots, m} \max_{\|y-x\| \leq \delta} b_i + (a^i)^T y \\ &= \max_{i=1, \dots, m} \max_{\|d\| \leq \delta} b_i + (a^i)^T (x + d) \\ &= \max_{i=1, \dots, m} (b_i + \delta \|a^i\|_*) + (a^i)^T x, \end{aligned} \quad (5)$$

where $\|\cdot\|_*$ is the dual norm of $\|\cdot\|$. Therefore the FA optimization problem can be written as:

$$\min_{x \in \mathbb{R}^n} \tilde{f}(x) = \min_{x \in \mathbb{R}^n} \max_{i=1, \dots, m} (b_i + \delta \|a^i\|_*) + (a^i)^T x. \quad (6)$$

The functional form of $\tilde{f}(\cdot)$ is structurally identical to that of $f(\cdot)$, namely the maximum of m linear functions, and both $f(\cdot)$ and $\tilde{f}(\cdot)$ are convex functions. Let us presume that it is easy to compute the dual norm $\|a\|_*$ for any a . Under this presumption the computation of $\tilde{f}(\cdot)$ will be as

easy as that of $f(\cdot)$ and computing a subgradient of $\tilde{f}(\cdot)$ at a given value of x will be as easy as that of $f(\cdot)$. Furthermore, it is reasonable to expect that any algorithm for minimizing $f(\cdot)$ in (4) should be easy to apply to solve (6) with similar types of computational guarantees.

The second class of examples are instances where $S = \mathbb{R}^n$ and $f(x) = \|Ax + b\|_2$ or $f(x)$ is a strictly convex quadratic function, and the prescribed norm on the space of variables x is the Euclidean norm $\|x\|_2$. In these cases, Lewis (2002) shows that the resulting fabrication-adaptive optimization problem (3) can be modeled using semidefinite optimization.

The third class of examples are instances of the maximum eigenvalue function where $S = \mathbb{R}^n$. Given symmetric matrices A_0, A_1, \dots, A_n , let $\mathcal{A}(x) := A_0 + \sum_{i=1}^n A_i x_i$ and consider the maximum eigenvalue function $f(\cdot) : \mathbb{R}^n \rightarrow \mathbb{R}$ given by:

$$f(x) := \lambda_{\max}(\mathcal{A}(x)) .$$

Note that $f(\cdot)$ is convex on \mathbb{R}^n , and $f(\cdot)$ generalizes the maximum of linear functions. (Indeed, $f(\cdot)$ specializes to the maximum of linear functions when all matrices A_0, A_1, \dots, A_n are diagonal.) The fabrication-adaptive counterpart function $\tilde{f}(\cdot)$ of $f(\cdot)$ is

$$\tilde{f}(x) = \max_{y \in S, \|y-x\| \leq \delta} \lambda_{\max}(\mathcal{A}(y)) , \quad (7)$$

and $\tilde{f}(\cdot)$ is also a convex function when $S = \mathbb{R}^n$ from Proposition 3.1 of Lewis (2002). However, there does not appear to be any efficient method for computing $\tilde{f}(\cdot)$ even in the case when $S = \mathbb{R}^n$ unless the norm $\|\cdot\|$ has very special structure. When $\|\cdot\| = \|\cdot\|_1$, then the unit ball is the convex hull of the $2n$ signed unit vectors $e^1, \dots, e^n, -e^1, \dots, -e^n$, whereby $\tilde{f}(x)$ can be computed as:

$$\tilde{f}(x) = \max_{j=1, \dots, n} \{ \lambda_{\max}(\mathcal{A}(x + \delta e^j)), \lambda_{\max}(\mathcal{A}(x - \delta e^j)) \} ,$$

and so is computable so long as the $2n$ largest eigenvalue problems are efficiently computable. However, when $\|\cdot\| = \|\cdot\|_\infty$, it follows from Ben-tal and Nemirovski (2002) that computing $\tilde{f}(\cdot)$ is NP-hard, and when $\|\cdot\| = \|\cdot\|_2$, computing $\tilde{f}(\cdot)$ is also NP-hard (Nemirovski 2012). Here we see that the original objective function $f(\cdot)$ involves the computation of the largest eigenvalue of a symmetric matrix, which is typically tractable; however the FA counterpart function $\tilde{f}(\cdot)$ is not tractable to compute when $\|\cdot\| = \|\cdot\|_p$ and $p = 2$ or $p = \infty$. Indeed, intuition suggests that only norms with a relatively small number of extreme points on their unit ball will be suitable for practical computation of the FA counterpart of the largest eigenvalue function.

2.2. Piecewise linear convex objective and $S \neq \mathbb{R}^n$

Let the objective function be given by (4), i.e., the same as in Subsection 2.1, but now suppose that $S \neq \mathbb{R}^n$. For convenience we assume in this subsection that S is closed and bounded, i.e., compact. Then we have:

$$\begin{aligned} \tilde{f}(x) &= \max_{y \in S, \|y-x\| \leq \delta} \max_{i=1, \dots, m} b_i + (a^i)^T y \\ &= \max_{i=1, \dots, m} \max_{y \in S, \|y-x\| \leq \delta} b_i + (a^i)^T y \\ &= \max_{i=1, \dots, m} \tilde{f}_i(x) , \end{aligned} \quad (8)$$

where

$$\begin{aligned} \tilde{f}_i(x) &:= \max_y b_i + (a^i)^T y \\ \text{s.t. } &\|y - x\| \leq \delta \\ &y \in S . \end{aligned} \quad (9)$$

We have the following result on the structure of $\tilde{f}(\cdot)$:

PROPOSITION 1. *If S is a convex set, then $\tilde{f}_i(\cdot) : S \rightarrow \mathbb{R}$ is a concave function, $i = 1, \dots, m$, whereby $\tilde{f}(\cdot)$ is the pointwise maximum of concave functions.*

Proof: Let us fix $i \in \{1, \dots, m\}$, and let $x^1, x^2 \in S$ be given. Let $\alpha \in [0, 1]$, and $x^3 = \alpha x^1 + (1 - \alpha)x^2$. Assuming for simplicity that the optimization problem defining $\tilde{f}_i(x)$ attains its optimum, let y^j solve the optimization problem in the definition of $\tilde{f}_i(x^j)$ for $j = 1, 2$, whereby $\tilde{f}_i(x^j) = b_i + (a^i)^T y^j$, $y^j \in S$, and $\|x^j - y^j\| \leq \delta$ for $j = 1, 2$. Therefore $y^3 := \alpha y^1 + (1 - \alpha)y^2$ satisfies $y^3 \in S$, and $\|x^3 - y^3\| \leq \delta$ and hence y^3 is feasible for the optimization problem in the definition of $\tilde{f}_i(x^3)$ in (9). Therefore $\tilde{f}_i(x^3) \geq b_i + (a^i)^T y^3 = \alpha(b_i + (a^i)^T y^1) + (1 - \alpha)(b_i + (a^i)^T y^2) = \alpha \tilde{f}_i(x^1) + (1 - \alpha)\tilde{f}_i(x^2)$, and hence $\tilde{f}_i(\cdot)$ is concave on S . \square

It follows from Proposition 1 that $\tilde{f}(\cdot)$ does not have attractive convex structure. Nevertheless, the computation of $\tilde{f}(x)$ for a given x via (8)-(9) is a tractable convex optimization problem when $\|\cdot\|$ is the L_2 , L_1 , or L_∞ norm, and when S is polyhedral or is conveyed in a suitably easy conic form $S = \{x : b - Ax \in K\}$ for some convex cone K . In these cases, computing $\tilde{f}(x)$ amounts to solving m conic convex optimization problems. This is not a particularly burdensome task if m is not too large, and/or if S is a relatively simple set such as a hypercube, simplex, or Euclidean ball, or more generally if S is conveyed in conic form above with structure for which conic optimization can be done efficiently.

Using (8) and (9), the FA optimization problem (3) can therefore be written as:

$$\begin{aligned} P^{\text{FA}} : \quad \tilde{z}^* := \min_x \tilde{f}(x) &= \min_{x,t} t \\ \text{s.t. } x \in S &\quad \text{s.t. } \tilde{f}_i(x) \leq t, \quad i = 1, \dots, m \\ &\quad x \in S. \end{aligned} \quad (10)$$

Furthermore, we know from Proposition 1 that $\tilde{f}_i(\cdot)$ is concave, $i = 1, \dots, m$.

In light of the structure of the FA optimization problem (10), we consider computing first-order objects for each of the functions $\tilde{f}_i(x)$, $i = 1, \dots, m$. Let us fix an index $i \in \{1, \dots, m\}$. We know from Proposition 1 that $\tilde{f}_i(\cdot)$ is concave on S and hence has a subgradient for all $x \in S$. Furthermore, there exists a set $B_i \subset S$ of measure zero such that $\tilde{f}_i(\cdot)$ will be differentiable for all $x \in S \setminus B_i$ (Rockafellar (1970), Theorem 25.5). To see how to compute such a subgradient we appeal to duality theory and we assume that S is conveyed in conic form, namely $S = \{x \in \mathbb{R}^n : b - Ax \in K\}$ where $K \subset \mathbb{R}^k$ is a closed convex cone. For $i = 1, \dots, m$, we can re-write (9) as the following problem $P_i(x)$:

$$\begin{aligned} P_i(x) : \quad \tilde{f}_i(x) = \max_y \quad & b_i + (a^i)^T y \\ \text{s.t.} \quad & \|y - x\| \leq \delta \\ & b - Ay \in K, \end{aligned} \quad (11)$$

which can be put in conic form by defining $C := \{(w, \alpha) : \|w\| \leq \alpha\} \times K$ and re-writing $P_i(x)$ as:

$$\begin{aligned} P_i(x) : \quad \tilde{f}_i(x) = \max_y \quad & b_i + (a^i)^T y \\ \text{s.t.} \quad & \begin{pmatrix} x \\ \delta \\ b \end{pmatrix} - \begin{pmatrix} I \\ 0 \\ A \end{pmatrix} y \in C. \end{aligned} \quad (12)$$

The conic dual $D_i(x)$ of $P_i(x)$ can then be written as:

$$\begin{aligned} D_i(x) : \min_{\pi} \quad & b_i + \delta \|a^i - A^T \pi\|_* + b^T \pi + (a^i - A^T \pi)^T x \\ \text{s.t.} \quad & \pi \in K^*. \end{aligned} \quad (13)$$

We say that S has a *Slater point* if there exists $x^0 \in S$ for which $b - Ax^0 \in \text{int}K$. The following result describes a way to compute a subgradient of $\tilde{f}_i(x)$:

PROPOSITION 2. Let $i \in \{1, \dots, m\}$ be given. Suppose that S has a Slater point, and suppose $x \in S$. Then $D_i(x)$ attains its optimum at some π_i^* with no duality gap, and furthermore

$$p_i := p_i(x) := a^i - A^T \pi_i^* \quad (14)$$

is a subgradient of $\tilde{f}_i(\cdot)$ at x . Furthermore, there is a set $B_i \subset S$ of measure zero for which it holds that $p_i(x)$ is uniquely defined and hence $\nabla \tilde{f}_i(x) = p_i(x)$ for all $x \in S \setminus B_i$.

Proof: Let us fix $i \in \{1, \dots, m\}$ and consider the duality paired problems $P_i(x)$ and $D_i(x)$. It follows from standard duality theory that there will be no duality gap and the dual problem will attain its optimum under the condition that the primal has a Slater point, namely a point y for which $\|y - x\| < \delta$ and $b - Ay \in \text{int}K$; see Duffin (1956) or Borwein and Lewis (2006) for a more modern treatment of conic duality. Let x^0 be a Slater point of S , whereby $b - Ax^0 \in \text{int}K$. Since $x \in S$ by supposition, it follows that $y(\varepsilon) := \varepsilon x^0 + (1 - \varepsilon)x$ is a Slater point of the feasible region of (12) for all $\varepsilon > 0$ and sufficiently small. It then follows that $D_i(x)$ attains its optimum with no duality gap, and it follows from the formulation of $D_i(x)$ that $\tilde{f}_i(x)$ is the pointwise minimum of affine functions, whose linear terms are of the form $(a^i - A^T \pi)$ for $\pi \in K^*$. It then follows directly from convexity arguments that $a^i - A^T \pi_i^*$ is a subgradient of $\tilde{f}_i(\cdot)$ at x . Furthermore, it follows from Rockafellar (1970) (Theorem 25.5) that there exists a set $B_i \subset S$ of measure zero such that $\tilde{f}_i(\cdot)$ is differentiable for all $x \in S \setminus B_i$, and hence $\nabla \tilde{f}_i(x) = p_i(x)$ for all $x \in S \setminus B_i$. \square

The computational viability of solving the dual problem $D_i(x)$ must of necessity presume that the dual norm $\|\cdot\|_*$ can be suitably treated in the objective function of $D_i(x)$. Of course, when the norm $\|\cdot\|$ can be described with linear inequalities or second-order cone constraints, then solving $D_i(x)$ is all the more easy. For example, when $\|\cdot\|$ is the L_1 - or L_∞ -norm, then $D_i(x)$ can be easily represented as a linear programming problem. When $\|\cdot\|$ is the L_2 -norm or other quadratic norm of the form $\sqrt{x^T Q x}$ for $Q \succ 0$, then $D_i(x)$ can be represented as a second-order cone problem using a standard transformation, see Boyd and Vandenberghe (2004).

In Section 2.4 we will present an algorithm for solving (10) that is based on the scheme of sequentially solving the first-order approximation of (10) at a given point $\hat{x} \in S$, namely:

$$\begin{aligned} P^{\hat{x}} : \min_{x,t} \quad & t \\ \text{s.t.} \quad & \tilde{f}_i(\hat{x}) + \nabla \tilde{f}_i(\hat{x})^T (x - \hat{x}) \leq t, \quad i = 1, \dots, m \\ & x \in S, \end{aligned} \quad (15)$$

where the values $\tilde{f}_i(\hat{x})$ and $\nabla \tilde{f}_i(\hat{x})$, $i = 1, \dots, m$, are computed via Propositions 1 and 2, respectively.

2.3. Linear fractional objective and $S \neq \mathbb{R}^n$

Let us now consider the case when the objective function is linear fractional:

$$f(x) := \frac{a^T x + g}{c^T x + h}, \quad (16)$$

and suppose that $S \neq \mathbb{R}^n$ and we impose the condition that S is compact and convex, and $c^T x + h > 0$ for all $x \in S$. In this case $f(\cdot)$ is quasilinear on S , i.e., it is both quasiconvex and quasiconcave on S . We can write the fabrication-adaptive objective function as:

$$\begin{aligned} \tilde{f}(x) := \max_y \quad & \frac{a^T y + g}{c^T y + h} \\ \text{s.t.} \quad & \|y - x\| \leq \delta \\ & y \in S. \end{aligned} \quad (17)$$

We have the following result on the structure of $\tilde{f}(\cdot)$:

PROPOSITION 3. $\tilde{f}(\cdot) : S \rightarrow \mathbb{R}$ is a quasiconcave function on S .

Proof: Let $x^1, x^2 \in S$ be given, let $\alpha \in [0, 1]$, and let $x^3 = \alpha x^1 + (1 - \alpha)x^2$. Let y^j solve the optimization problem in the definition of $\tilde{f}(x^j)$ in (17) for $j = 1, 2$, whereby $\|x^j - y^j\| \leq \delta$, $y^j \in S$, and $\frac{a^T y^j + g}{c^T y^j + h} = \tilde{f}(x^j)$ for $j = 1, 2$. Define $\beta := \min\{\tilde{f}(x^1), \tilde{f}(x^2)\}$. Then the equations $\tilde{f}(x^j) = \frac{a^T y^j + g}{c^T y^j + h}$ for $j = 1, 2$ and the definition of β implies that $a^T y^j + g = \tilde{f}(x^j)[c^T y^j + h] \geq \beta[c^T y^j + h]$ for $j = 1, 2$. Also $y^3 := \alpha y^1 + (1 - \alpha)y^2$ satisfies $y^3 \in S$ and $\|x^3 - y^3\| \leq \delta$ and hence is feasible for the optimization problem in the definition of $\tilde{f}(x^3)$ in (17). Furthermore $a^T y^3 + g \geq \beta[c^T y^3 + h]$, and hence $\tilde{f}(x^3) \geq \beta = \min\{\tilde{f}(x^1), \tilde{f}(x^2)\}$, whereby $\tilde{f}(\cdot)$ is quasiconcave on S . \square

The next result shows that $\tilde{f}(x)$ is the optimal objective function value of a convex optimization problem involving S and a norm constraint. In what follows we use the notation that θS is the scaling of S by the constant θ for $\theta \geq 0$. (When $\theta = 0$, it is customary to define θS to be the recession cone of S ; however since we assume here that S is bounded we have for $\theta = 0$ that $\theta S := \{0\}$ under either definition.)

PROPOSITION 4. If $x \in S$, then $\tilde{f}(x)$ is the optimal objective value of the following convex optimization problem:

$$\begin{aligned} \tilde{f}(x) := & \max_{\bar{y}, \theta} a^T \bar{y} + g\theta \\ \text{s.t. } & \|\bar{y} - \theta x\| \leq \theta\delta \\ & c^T \bar{y} + h\theta = 1 \\ & \bar{y} \in \theta S \\ & \theta \geq 0. \end{aligned} \tag{18}$$

If (\bar{y}, θ) is feasible and/or optimal for (18), then $y = \bar{y}/\theta$ is feasible and/or optimal for (17), respectively.

Proof: Problem (18) is just a standard transformation of the linear fractional optimization problem (17) via homogenization (see Charnes and Cooper (1962) or Craven and Mond (1973)). Note that we cannot have $\theta = 0$ in (18), as this would imply that $\bar{y} = 0$ via the norm constraint, which would imply that $c^T \bar{y} + h\theta = 0 \neq 1$, which is a contradiction. Thus division by zero in the transformation $y = \bar{y}/\theta$ cannot occur. \square

The computational viability of solving (18) will depend on (among other things) the ability to conveniently work with the scaling θS . When S is conveyed in conic linear form as in Section 2.2, it follows for $\theta \geq 0$ that $\theta S = \{x \in \mathbb{R}^n : \theta b - Ax \in K\}$, in which case the scaling results in no loss of generality of the representation of the feasible region.

Let us now turn to the computation of first-order objects related to $\tilde{f}(\cdot)$. Let us further assume that S is conveyed as a system of linear inequalities, so that $S = \{x \in \mathbb{R}^n : b - Ax \geq 0\}$, i.e., $K = \mathbb{R}_+^k$ in the conic linear representation. We then can write (18) as:

$$\begin{aligned} \tilde{f}(x) := & \max_{\bar{y}, \theta} a^T \bar{y} + g\theta \\ \text{s.t. } & \|\bar{y} - \theta x\| \leq \theta\delta \\ & c^T \bar{y} + h\theta = 1 \\ & \theta b - A\bar{y} \geq 0 \\ & \theta \geq 0. \end{aligned} \tag{19}$$

Let us further restrict our attention to the case when the norm $\|\cdot\|$ is representable with linear inequalities, as in the L_1 - or L_∞ -norm. For concreteness let us examine the case when $\|\cdot\|$ is a weighted L_1 -norm with weights $w := (w_1, \dots, w_n) > 0$, i.e., $\|x\| := \sum_{j=1}^n w_j |x_j|$. Then (19) can be represented as the following linear optimization problem:

$$\begin{aligned}
 \tilde{f}(x) := \max_{\bar{y}, \theta, q} \quad & a^T \bar{y} + g\theta \\
 \text{s.t.} \quad & \bar{y} - \theta x \leq q \quad (\pi_1) \\
 & -\bar{y} + \theta x \leq q \quad (\pi_2) \\
 & w^T q \leq \theta \delta \quad (\gamma) \\
 & c^T \bar{y} + h\theta = 1 \quad (\tau) \\
 & \theta b - A\bar{y} \geq 0 \quad (\lambda) \\
 & \theta \geq 0 \quad , \quad (\kappa)
 \end{aligned} \tag{20}$$

where for future reference we assign names of linear optimization dual variables for each of the constraint systems above. We have the following result concerning the computation of the gradient of $\tilde{f}(\cdot)$:

PROPOSITION 5. *There is a set $B \subset S$ of measure zero which makes the following hold: suppose $x \in S \setminus B$, and let $(\bar{y}^*, \theta^*, q^*)$ solve (20) and let $(\pi_1^*, \pi_2^*, \gamma^*, \tau^*, \lambda^*, \kappa^*)$ be optimal dual variables, and define:*

$$p := p(x) := \theta^*(\pi_1^* - \pi_2^*) . \tag{21}$$

Then $\nabla \tilde{f}(x) = p(x)$.

Below we present a proof of Proposition 5. This proof relies on (20) being a linear optimization problem. This will be the case whenever S is conveyed via linear inequalities, and whenever the norm $\|\cdot\|$ is polyhedral, or to be more exact, whenever the norm level set constraint “ $\|v\| \leq t$ ” in variables v, t can be conveniently represented via linear inequalities. While we specifically worked with the weighted L_1 -norm in (20), there is no loss of generality in working with a weighted L_∞ -norm or other polyhedral norm.

As (20) is a linear program parameterized by x , it would be convenient to prove Proposition 5 by invoking a standard right-hand-side sensitivity analysis result on parametric linear programming. However, notice that the parameter x appears in the left-hand-side of the first two constraints of (20), and this dependence of the constraint-matrix coefficients of (20) on the parameter x appears to be structural, i.e., we see no way to remove it by a simple change of variable. Thus to prove Proposition 5 we will invoke the following result concerning changes in data coefficients in linear programming:

THEOREM 1. *Consider the following primal and dual pair of linear optimization problems:*

$$\begin{aligned}
 P(x) : f(x) = \min_y \quad & c_x^T y \\
 \text{s.t.} \quad & A_x y = b_x, \\
 & y \geq 0. \\
 D(x) : \max_z \quad & b_x^T z \\
 \text{s.t.} \quad & A_x^T z \leq c_x, \\
 & z \text{ free.}
 \end{aligned} \tag{22}$$

Suppose $A_x = A_0 + \sum_{k=1}^{n_x} A_k x_k$, $b_x = b_0 + \sum_{k=1}^{n_x} b_k x_k$, and $c_x = c_0 + \sum_{k=1}^{n_x} c_k x_k$, where $x = (x_1, x_2, \dots, x_{n_x})$ are parameters that determine the data A_x, b_x, c_x of the linear program $P(x)$. Let S denote the subset of \mathbb{R}^{n_x} for which $P(x)$ has an optimal solution. Then there exists a set $B \subset S$ of measure zero which makes the following hold: if $\hat{x} \in S \setminus B$, and y^*, z^* are optimal solutions to $P(\hat{x})$ and $D(\hat{x})$, then

$$\left. \frac{\partial f(x)}{\partial x_k} \right|_{x_k = \hat{x}_k} = c_k^T y^* + b_k^T z^* - (z^*)^T A_k y^*. \tag{23}$$

Theorem 1 follows as the multivariate extension of the case when $n_x = 1$ using rational functions (see Lemma 1 and Theorem 2 of Freund (1985)). \square

Proof of Proposition 5: The proof follows by applying Theorem 1 in the linear optimization problem (20). Considering the k^{th} component of x we have from Theorem 1 that

$$\left. \frac{\partial \tilde{f}(x)}{\partial x_k} \right|_{x_k} = \theta^*(\pi_1^*)_k - \theta^*(\pi_2^*)_k ,$$

except possibly on a set B of measure zero, which proves the result. \square

2.4. Piecewise-linear fractional objective and $S \neq \mathbb{R}^n$

Let us now consider the case when the objective function is piecewise-linear fractional:

$$f(x) := \max_{i=1, \dots, m} \frac{(a^i)^T x + g_i}{(c^i)^T x + h_i} , \quad (24)$$

and we impose the conditions that S is compact and convex, and $(c^i)^T x + h_i > 0$ for all $x \in S$ and for all $i = 1, \dots, m$.

Similar to Section 2.3, it holds that $f(\cdot)$ is quasiconvex on S (but not quasiconcave). We can write the FA objective function as:

$$\begin{aligned} \tilde{f}(x) &= \max_{y \in S, \|y-x\| \leq \delta} \max_{i=1, \dots, m} \frac{(a^i)^T y + g_i}{(c^i)^T y + h_i} \\ &= \max_{i=1, \dots, m} \max_{y \in S, \|y-x\| \leq \delta} \frac{(a^i)^T y + g_i}{(c^i)^T y + h_i} \\ &= \max_{i=1, \dots, m} \tilde{f}_i(x) , \end{aligned} \quad (25)$$

where

$$\begin{aligned} \tilde{f}_i(x) &:= \max_y \frac{(a^i)^T y + g_i}{(c^i)^T y + h_i} \\ \text{s.t. } &\|y - x\| \leq \delta \\ &y \in S . \end{aligned} \quad (26)$$

The following result on the structure of $\tilde{f}(\cdot)$ is evident from Proposition 3:

PROPOSITION 6. $\tilde{f}_i(\cdot) : S \rightarrow \mathbb{R}$ is a quasiconcave function, $i = 1, \dots, m$, whereby $\tilde{f}(\cdot)$ is the pointwise maximum of quasiconcave functions.

Proof: The proof is an immediate consequence of Proposition 3. \square

Paralleling results in Section 2.3, we have the following result on the computation of $\tilde{f}(\cdot)$, which shows that $\tilde{f}(\cdot)$ is computable by solving m convex optimization problems.

PROPOSITION 7. If $x \in S$, then $\tilde{f}(x) = \max_{i=1, \dots, m} \tilde{f}_i(x)$ where for $i = 1, \dots, m$, $\tilde{f}_i(x)$ is the optimal objective function value of the following convex optimization problem:

$$\begin{aligned} P_i(x) : \quad \tilde{f}_i(x) &:= \max_{\bar{y}, \theta} (a^i)^T \bar{y} + g_i \theta \\ \text{s.t. } &\|\bar{y} - \theta x\| \leq \theta \delta \\ &(c^i)^T \bar{y} + h_i \theta = 1 \\ &\bar{y} \in \theta S \\ &\theta \geq 0 . \end{aligned} \quad (27)$$

For each $i = 1, \dots, m$, if (\bar{y}, θ) is feasible and/or optimal for $P_i(x)$ in (27), then $y = \bar{y}/\theta$ is feasible and/or optimal for (26), respectively.

Proof: Proposition 7 is essentially a restatement of Proposition 4 for each of the $i = 1, \dots, m$ pieces $\tilde{f}_i(\cdot)$ of $\tilde{f}(\cdot)$. \square

As in Section 2.2, using (25) and (26) the FA optimization problem (3) can be written as:

$$P^{\text{FA}} : \quad \begin{aligned} \tilde{z}^* := \min_x \quad & \tilde{f}(x) &= \min_{x,t} \quad & t \\ \text{s.t.} \quad & x \in S & \text{s.t.} \quad & \tilde{f}_i(x) \leq t, \quad i = 1, \dots, m \\ & & & x \in S. \end{aligned} \quad (28)$$

Furthermore, we know from Proposition 6 that $\tilde{f}_i(\cdot)$ is quasiconcave, $i = 1, \dots, m$.

Let $\hat{x} \in S$ be a given point. In light of the structure of the fabrication-adaptive optimization problem (28), we consider computing first-order objects for each of the functions $\tilde{f}_i(x)$, $i = 1, \dots, m$. Similar to Section 2.3, we assume that S is conveyed as a system of k linear inequalities, namely $S = \{x \in \mathbb{R}^n : b - Ax \geq 0\}$, i.e., $K = \mathbb{R}_+^k$ in the conic linear representation, and in particular we examine the case when the prescribed norm is the weighted L_1 -norm with weights $w := (w_1, \dots, w_n) > 0$. Then for $i = 1, \dots, m$, problem (27) can be represented as the following linear optimization problem:

$$P_i(x) : \quad \begin{aligned} \tilde{f}_i(x) := \max_{\bar{y}_i, \theta_i, q_i} \quad & (a^i)^T \bar{y}_i + g_i \theta_i \\ \text{s.t.} \quad & \bar{y}_i - \theta_i x \leq q_i & (\pi_{i,1}) \\ & -\bar{y}_i + \theta_i x \leq q_i & (\pi_{i,2}) \\ & w^T q_i \leq \theta_i \delta & (\gamma_i) \\ & (c^i)^T \bar{y}_i + h_i \theta_i = 1 & (\tau_i) \\ & \theta b - A \bar{y}_i \geq 0 & (\lambda_i) \\ & \theta_i \geq 0, & (\kappa_i) \end{aligned} \quad (29)$$

where for future reference we assign names of linear optimization dual variables for each of the constraint systems above. The analogous result of Proposition 5 is:

PROPOSITION 8. *Let $i \in \{1, \dots, m\}$ be given. There is a set $B_i \subset S$ of measure zero which makes the following hold: suppose $x \in S \setminus B_i$. Let $(\bar{y}_i^*, \theta_i^*, q_i^*)$ solve $P_i(x)$ of (29) and let $(\pi_{i,1}^*, \pi_{i,2}^*, \gamma_i^*, \tau_i^*, \lambda_i^*, \kappa_i^*)$ be optimal dual variables, and define:*

$$p_i := p_i(x) := \theta_i^* (\pi_{i,1}^* - \pi_{i,2}^*). \quad (30)$$

Then $\nabla \tilde{f}_i(x) = p_i(x)$.

Proof: The result follows directly from Proposition 5. \square

Based on Propositions 7 and 8, we propose an algorithm for solving the FA optimization problem P^{FA} in (28). Let $\hat{x} \in S$ be a given point. We sequentially solve the first-order approximation of (28) based on the point \hat{x} , namely:

$$P^{\hat{x}} : \quad \begin{aligned} \min_{x,t} \quad & t \\ \text{s.t.} \quad & \tilde{f}_i(\hat{x}) + \nabla \tilde{f}_i(\hat{x})^T (x - \hat{x}) \leq t, \quad i = 1, \dots, m \\ & x \in S, \end{aligned} \quad (31)$$

where the values $\tilde{f}_i(\hat{x})$ and $\nabla \tilde{f}_i(\hat{x})$, $i = 1, \dots, m$ are computed via Propositions 7 and 8, respectively. This leads to the sequential linear optimization scheme described in Table 1, which we refer to as Algorithm FA (for Fabrication-Adaptivity).

Table 1 Algorithm for fabrication-adaptive optimization problem when $f(\cdot)$ is piecewise linear fractional and S is given by linear inequalities.

Algorithm FA when $f(\cdot)$ is Piecewise Linear Fractional Problem	
Step 1.	Start with initial guess $\hat{x} := x^0$ and tolerance ϵ_{tol}
Step 2.	For each $i = 1, \dots, m$, do: Compute function value $\tilde{f}_i(\hat{x})$ via (29) Compute first-order information $p_i(\hat{x})$ via (30)
Step 3.	Form the linear optimization problem $P^{\hat{x}}$ in (31)
Step 4.	Solve $P^{\hat{x}}$ for an optimal solution x^*
Step 5.	If $\ x^* - \hat{x}\ \leq \epsilon_{\text{tol}}$, stop. Else update $\hat{x} \leftarrow x^*$ and go to Step 2.

Note that Algorithm FA is designed for the case when $f(\cdot)$ is piecewise linear fractional (24). When the denominators in the linear fractional forms are all equal to 1, i.e., $c^i = 0$ and $h_i = 1$ for $i = 1, \dots, m$, then it follows from Proposition 1 that $\tilde{f}_i(\cdot)$ is concave on S , whereby for $\hat{x} \in S$ we have:

$$\tilde{f}_i(x) \leq \tilde{f}_i(\hat{x}) + \nabla \tilde{f}_i(\hat{x})^T (x - \hat{x}) \text{ for all } x \in S, i = 1, \dots, m.$$

This in turn implies that if (x, t) is feasible for $P^{\hat{x}}$ (31), then (x, t) is also feasible for P^{FA} (28), whereby the optimal value of $P^{\hat{x}}$ will always be an upper bound on the value of P^{FA} in this case.

When we discuss bandgap optimization problems in Section 3 (for which the concept of fabrication adaptivity was originally inspired), we will show that the original bandgap optimization problem can be cast as an instance of the piecewise linear fractional optimization problem (24), and that Algorithm FA can therefore be used to solve the FA optimization problem associated with this problem. We will show computational results for a particularly useful bandgap optimization problem, namely the photonic crystal design problem, in Section 4.

2.5. A Very Special Piecewise Linear Fractional Problem

Let us now consider the following very special piecewise linear fractional objective function:

$$f(x) := \frac{\max_{i \in \mathcal{I}}((a^i)^T x + g_i) - \min_{j \in \mathcal{J}}((c^j)^T x + h_j)}{\max_{i \in \mathcal{I}}((a^i)^T x + g_i) + \min_{j \in \mathcal{J}}((c^j)^T x + h_j)}. \quad (32)$$

Similar in spirit to Section 2.4, we suppose that S is compact and convex, and we impose the condition that $(a^i)^T x + g_i > 0$ and $(c^j)^T x + h_j > 0$ for all $x \in S$, $i \in \mathcal{I}$, and $j \in \mathcal{J}$. Optimization problems with this structure arise naturally and often in bandgap optimization applications, which will be discussed in Section 3. (Indeed, bandgap optimization problems gave rise to our interest in this particular structure to begin with.)

In order to analyze the properties of $f(\cdot)$ as well as the fabrication-adaptive objective $\tilde{f}(\cdot)$ we will use the following result.

PROPOSITION 9. Suppose that $(a^i)^T x + g_i > 0$ and $(c^j)^T x + h_j > 0$ for all $x \in S$, $i \in \mathcal{I}$, and $j \in \mathcal{J}$. Then

$$f(x) := \frac{\max_{i \in \mathcal{I}}((a^i)^T x + g_i) - \min_{j \in \mathcal{J}}((c^j)^T x + h_j)}{\max_{i \in \mathcal{I}}((a^i)^T x + g_i) + \min_{j \in \mathcal{J}}((c^j)^T x + h_j)} = \max_{i \in \mathcal{I}, j \in \mathcal{J}} \frac{((a^i)^T x + g_i) - ((c^j)^T x + h_j)}{((a^i)^T x + g_i) + ((c^j)^T x + h_j)}. \quad (33)$$

Proof: To ease the notational burden let $U_i = (a^i)^T x + g_i$ for $i \in \mathcal{I}$ and $L_j = (c^j)^T x + h_j$ for $j \in \mathcal{J}$. Let us also define the general function $\phi(U, L) := \frac{U-L}{U+L}$, and notice that $\phi(\cdot, \cdot)$ is increasing in U and decreasing in L for $U > 0$ and $L > 0$. For a given value of $x \in S$, let us consider the left side and the right side of the equality (33) we need to prove. Clearly the right side is at least as large as the left side. Now suppose that (\hat{i}, \hat{j}) is a pair of indices that attains the maximum in the right side of (33). Then we have from the monotonicity of $\phi(U, L)$ that

$$\frac{\max_{i \in \mathcal{I}} U_i - \min_{j \in \mathcal{J}} L_j}{\max_{i \in \mathcal{I}} U_i + \min_{j \in \mathcal{J}} L_j} \geq \frac{U_{\hat{i}} - \min_{j \in \mathcal{J}} L_j}{U_{\hat{i}} + \min_{j \in \mathcal{J}} L_j} \geq \frac{U_{\hat{i}} - L_{\hat{j}}}{U_{\hat{i}} + L_{\hat{j}}},$$

thus showing that the left side of (33) is at least as large as the right side, completing the proof. \square

Proposition 9 shows that $f(\cdot)$ can alternatively be rewritten as the maximum of $m := |\mathcal{I}| \cdot |\mathcal{J}|$ linear fractional functions (where $|\mathcal{K}|$ denotes the cardinality of the set \mathcal{K}), and so is an instance of the format (24), and hence all of the results of Section 2.4 apply herein.

Indeed, we can write the FA objective function as:

$$\begin{aligned} \tilde{f}(x) &= \max_{y \in S, \|y-x\| \leq \delta} \frac{\max_{i \in \mathcal{I}} ((a^i)^T y + g_i) - \min_{j \in \mathcal{J}} ((c^j)^T y + h_j)}{\max_{i \in \mathcal{I}} ((a^i)^T y + g_i) + \min_{j \in \mathcal{J}} ((c^j)^T y + h_j)} \\ &= \max_{y \in S, \|y-x\| \leq \delta} \max_{i \in \mathcal{I}, j \in \mathcal{J}} \frac{((a^i)^T y + g_i) - ((c^j)^T y + h_j)}{((a^i)^T y + g_i) + ((c^j)^T y + h_j)} \\ &= \max_{i \in \mathcal{I}, j \in \mathcal{J}} \max_{y \in S, \|y-x\| \leq \delta} \frac{(a^i - c^j)^T y + (g_i - h_j)}{(a^i + c^j)^T y + (g_i + h_j)} \\ &= \max_{i \in \mathcal{I}, j \in \mathcal{J}} \tilde{f}_{i,j}(x), \end{aligned} \tag{34}$$

where for $(i, j) \in \mathcal{I} \times \mathcal{J}$ we have:

$$\begin{aligned} \tilde{f}_{i,j}(x) &:= \max_y \frac{(a^i - c^j)^T y + (g_i - h_j)}{(a^i + c^j)^T y + (g_i + h_j)} \\ &\text{s.t.} \quad \|y - x\| \leq \delta \\ &\quad y \in S, \end{aligned} \tag{35}$$

which has the exact same format as (25) and (26) with a finite index set given by all pairs $(i, j) \in \mathcal{I} \times \mathcal{J}$. Therefore $\tilde{f}_{i,j}(\cdot)$ is quasiconcave and $\tilde{f}(\cdot)$ is the pointwise maximum of quasiconcave functions (Proposition 6), the computation of $\tilde{f}_{i,j}(x)$ for a given $x \in S$ is the solution of the convex optimization problem described in Proposition 7, and the computation of $\nabla \tilde{f}_{i,j}(x)$ for a given x is obtained from dual variables as described in Proposition 8. Furthermore, the algorithm presented in Section 2.4 can be applied to solve the FA optimization problem derived from the original objective function given in (32).

3. Fabrication Adaptivity for Bandgap Optimization Problems

The motivation for developing the fabrication adaptivity paradigm stemmed from work on bandgap design optimization, and more specifically on photonic crystal design optimization. The works of Cox and Dobson (2000), Kao et al. (2005), and Men et al. (2010, 2011) contain methods to optimize bandgaps for this class of problems, but of necessity none of these works address issues of fabricability. The chief goal of this paper is to construct and solve fabrication-adaptive optimization problems for this class of problems. In this section we first review bandgap optimization problems

in general, and we present the class of bandgap optimization models used in the previous work. We then show how to apply the fabrication-adaptive formulation to bandgap optimization problems. The presentation herein is at a high level, and properties are stated as summary results of previous work without proofs; for a more detailed presentation we refer the interested reader to Men et al. (2010).

3.1. Bandgap Optimization Problems

A *bandgap* is a concept that arises in many engineering applications. In semiconductor physics, an electron can sometimes transition from one energy state to another by a change in crystal momentum. An *energy bandgap* thus denotes a range of energy states that the electrons are forbidden to occupy despite any change in momentum (in the absence of any external excitation). Analogously, in photonic crystals (periodic optical nanostructures), photons can behave as waves, and propagate with certain frequencies through the bulk material at admissible wavevectors. A *frequency bandgap* is defined as the range of disallowed frequencies of the photons; if a photon is traveling according to a given wavevector, it will get attenuated within the crystal if it is propagating at any frequency within the frequency bandgap. The energy bandgap phenomenon has been used in applications such as insulators, laser diodes, solar cells, etc., while the frequency bandgap phenomenon has been used in applications such as frequency filters, waveguides, and optical buffers.

Bandgap optimization is the process of designing the composition and structure of a material to maximize a specific bandgap. The bandgap optimization problem is generally written as the following nonlinear non-convex eigenvalue-constrained optimization problem:

$$P: \max_{x \in S} \frac{\min_{k \in \mathcal{Q}} \lambda_{m+1}(k, x) - \max_{k \in \mathcal{Q}} \lambda_m(k, x)}{\frac{1}{2}(\min_{k \in \mathcal{Q}} \lambda_{m+1}(k, x) + \max_{k \in \mathcal{Q}} \lambda_m(k, x))} \quad (36)$$

$$\text{s.t. } \mathbf{A}(k, x)u_j(k, x) = \lambda_j(k, x)\mathbf{M}u_j(k, x), \quad j = m, m+1, \text{ for all } k \in \mathcal{Q}.$$

The decision variables of problem P are $x \in S \subset \mathbb{R}^{n_x}$, which represent the discretized material property of the design domain, as shown in the left of Figure 1. The objective of problem P is the eigenvalue *gap-midgap* ratio, which is defined as the difference between two prescribed consecutive eigenvalues divided by their mean (for scale invariance). The constraints of problem P are described in the equation line (36), which is shorthand for “for each k in the index set \mathcal{Q} , $\lambda_j(k, x)$ is the j^{th} ordered (generalized) eigenvalue (for $j = m, m+1$) of $\mathbf{A}(k, x)$ with respect to \mathbf{M} , for the given design variable x .” Here \mathcal{Q} is a particular governing index set, and is typically discretized to have the n_k values $\mathcal{Q} = \{k_1, \dots, k_{n_k}\}$, as shown in the right of Figure 1. (Indeed, in most bandgap problems \mathcal{Q} indexes a discretization of the wave vectors which lie on the boundary of the Brillouin zone.)

Much of the details and derivation of the generalized eigensystem equation of (36) are beyond the scope of the present paper. However, we call out certain properties of \mathbf{M} and the family of matrices $\mathbf{A}(k, x)$, as they are used in subsequent reformulations.

PROPOSITION 10. *Let $\lambda_1(k, x) \leq \lambda_2(k, x) \leq \dots \leq \lambda_N(k, x)$ denote the eigenvalues of the generalized eigensystem equation of (36), with corresponding normalized eigenfunctions $u_1(k, x), u_2(k, x), \dots, u_N(k, x)$. Then \mathbf{M} and $\mathbf{A}(k, x)$ have the following properties:*

- (i) $\mathbf{M} \succ 0$,
- (ii) $\mathbf{A}(k, x) \succeq 0$, for all $k \in \mathcal{Q}$, $x \in S$,
- (iii) $\mathbf{A}(k, x) = \mathbf{A}_0(k) + \sum_{i=1}^{n_x} \mathbf{A}_i(k) x_i$, for all $k \in \mathcal{Q}$,
- (iv) $\lambda_i(k, x) \geq 0$, for all $i = 1, \dots, N$, and
- (v) $u_i(k, x)^T \mathbf{M} u_j(k, x) = \delta_{ij}$, for all $i, j = 1, \dots, N$. \square

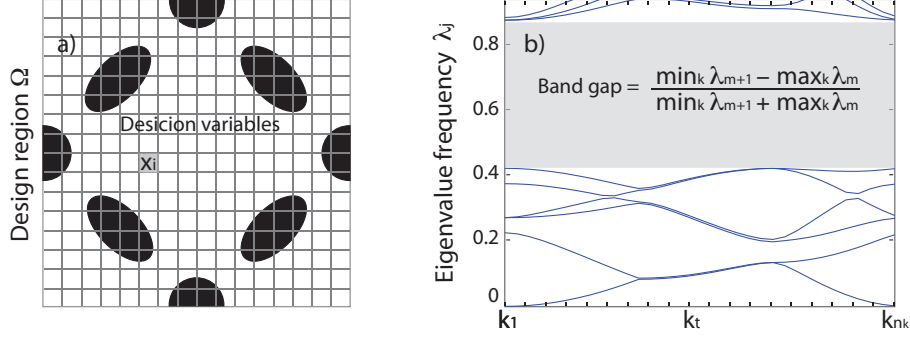


Figure 1 Bandgap optimization problem. The left figure is the schematic representation of the design problem. The design region is represented by piecewise constant values x_i of pixel (or voxel) i for each of $i = 1, \dots, n_x$ pixels, where x_i is the value of the material property of design interest (such as permittivity, Poisson's ratio, Young's modulus, etc.). The right figure is the band diagram: in this example \mathcal{Q} is the interval $[k_1, k_{n_k}]$, which is discretized into a finite number of components $\{k_1, \dots, k_{n_k}\}$. Each curve shows an eigenvalue parameterized over the elements of \mathcal{Q} . The band shown in the figure is the difference between the 6th and 7th eigenvalues, and portrays the numerator of the objective function in (36). The objective is to determine the values of the design variables x for which the resulting bandgap between these consecutive eigenvalues is largest.

Item (i) of Proposition 10 states that the (mass) matrix \mathbf{M} is positive definite, while item (ii) states that $\mathbf{A}(k, x)$ is positive semidefinite for any feasible design x , and for every $k \in \mathcal{Q}$. Item (iii) states that the matrix $\mathbf{A}(k, x)$ depends affinely on the design variables x , for every $k \in \mathcal{Q}$. Items (iv) and (v) state that the generalized eigenvalues are nonnegative and the generalized eigenfunctions are \mathbf{M} -orthogonal, which are direct consequences of the previous three items.

Now let $\hat{x} \in S$ be given. To ease the notation burden, we identify the finite set $\mathcal{Q} := \{k_1, \dots, k_{n_k}\}$ with the counter $t \in \{1, \dots, n_k\}$. In Men et al. (2010) it is shown how to construct operators $\mathcal{A}_{\ell,t}^{\hat{x}}(x) = A_{\ell,t,0}^{\hat{x}} + \sum_{i=1}^{n_x} A_{\ell,t,i}^{\hat{x}} x_i$ and $\mathcal{A}_{u,t}^{\hat{x}}(x) := A_{u,t,0}^{\hat{x}} + \sum_{i=1}^{n_x} A_{u,t,i}^{\hat{x}} x_i$, and also corresponding mass matrices $M_{\ell,t}^{\hat{x}}$ and $M_{u,t}^{\hat{x}}$, for each $t \in \{1, \dots, n_k\}$, all of whose data depends on the current point \hat{x} , which are used to construct the following (convex) linear fractional semidefinite optimization problem (SDP):

$$\begin{aligned}
 P_{SDP}^{\hat{x}} : \quad & \max_{x \in S, \lambda_{\ell}, \lambda_u} \quad 2 \frac{\lambda_u - \lambda_{\ell}}{\lambda_u + \lambda_{\ell}} \\
 \text{s.t.} \quad & \mathcal{A}_{\ell,t}^{\hat{x}}(x) \preceq \lambda_{\ell} M_{\ell,t}^{\hat{x}}, \quad t = 1, \dots, n_k, \\
 & \mathcal{A}_{u,t}^{\hat{x}}(x) \succeq \lambda_u M_{u,t}^{\hat{x}}, \quad t = 1, \dots, n_k, \\
 & \lambda_{\ell} \geq 0, \lambda_u \geq 0.
 \end{aligned} \tag{37}$$

PROPOSITION 11. *For a given $\hat{x} \in S$, the nonlinear nonconvex problem P is locally approximated as the (convex) linear fractional semidefinite program $P_{SDP}^{\hat{x}}$ of (37). \square*

Without going into the fine details, we note that λ_{ℓ} and λ_u in (37) are intended to model $\max_{k \in \mathcal{Q}} \lambda_m(k, x)$ and $\min_{k \in \mathcal{Q}} \lambda_{m+1}(k, x)$ in (36), respectively, and that the two pairs of semidefinite inclusions in (37) locally model the m^{th} and $(m+1)^{\text{st}}$ eigenvalue position for each $k \in \mathcal{Q} = \{k_1, \dots, k_{n_k}\}$.

Our goal herein is to apply the fabrication adaptivity paradigm to bandgap optimization problems. Note that the objective function of (37) is at least as challenging as the largest eigenvalue function of Section 2.1. Recall from the discussion in Section 2.1 that the fabrication-adaptive counterpart function of the largest eigenvalue function is typically not computationally tractable.

We therefore proceed by replacing the semidefinite inclusions in (37) with linear inequality approximations, the methodology for which is described in Appendix B.1, which yields the data $B^{\hat{x}}$, $C^{\hat{x}}$, $g^{\hat{x}}$, and $h^{\hat{x}}$ for the linear fractional optimization problem:

$$\begin{aligned} P_{LFP}^{\hat{x}} : \quad & \max_{x \in S, \lambda_\ell, \lambda_u} \quad 2 \frac{\lambda_u - \lambda_\ell}{\lambda_u + \lambda_\ell} \\ \text{s.t.} \quad & B^{\hat{x}}x + g^{\hat{x}} \leq e\lambda_\ell, \\ & C^{\hat{x}}x + h^{\hat{x}} \geq e\lambda_u, \\ & \lambda_\ell \geq 0, \lambda_u \geq 0. \end{aligned} \quad (38)$$

PROPOSITION 12. *For a given $\hat{x} \in S$, the linear fractional semidefinite program $P_{SDP}^{\hat{x}}$ of (37) is approximated as the linear fractional optimization problem $P_{LFP}^{\hat{x}}$ of (38). \square*

Here the two groups of semidefinite inclusions in (37) are replaced by \mathcal{N}_B and \mathcal{N}_C linear inequalities, respectively. The detailed methodology and derivation of the approximating linear inequalities are not the focus of the current work, but are nevertheless presented in Appendix B.1 for completeness. In addition, the computational results presented in Appendix B.3 show that solutions of (38) are nearly as good and often are superior to those of (37). Our methodology is similar in spirit to that of Serali and Fraticelli (2002), who replace semidefinite inclusions with linear inequalities to solve non-convex quadratic optimization problems on the simplex.

3.2. Fabrication Adaptivity Formulation

Notice that the linear fractional formulation in (38) can be equivalently written in the following format which emphasizes the special piecewise linear structure of the objective function:

$$\max_{x \in S} f^{\hat{x}}(x) := 2 \frac{\min_{i \in \mathcal{I}} (C^{\hat{x}}x + h^{\hat{x}})_i - \max_{j \in \mathcal{J}} (B^{\hat{x}}x + g^{\hat{x}})_j}{\min_{i \in \mathcal{I}} (C^{\hat{x}}x + h^{\hat{x}})_i + \max_{j \in \mathcal{J}} (B^{\hat{x}}x + g^{\hat{x}})_j}, \quad (39)$$

where $\mathcal{I} = \{1, \dots, \mathcal{N}_C\}$ and $\mathcal{J} = \{1, \dots, \mathcal{N}_B\}$. Note in (39) that the only constraint is the feasibility inclusion $x \in S$. This special piecewise linear fractional function is of the exact structure as the problem discussed in Section 2.5 (with the equivalence that now the objective is maximization rather than minimization and hence the roles of the “max” and “min” are switched in the fractional objective function). Furthermore, it will also be the case in the bandgap application that the suppositions of Section 2.5 are also satisfied, namely S is compact and is conveyed as a system of linear inequalities $S = \{x : Ax \leq b\}$, the norm $\|\cdot\|$ is a weighted 1-norm $\|x\| := \sum_{i=1}^{n_x} w_i |x_i|$ for positive weights (w_1, \dots, w_{n_x}) , and $(C^{\hat{x}}x + h^{\hat{x}})_i > 0$ and $(B^{\hat{x}}x + g^{\hat{x}})_j > 0$ for all $x \in S$ and $i \in \mathcal{I}$ and $j \in \mathcal{J}$, respectively. Therefore we can invoke the results in Section 2.5 regarding computation and optimization of the fabrication-adaptive counterpart function $\tilde{f}^{\hat{x}}(x)$. Let us see how this can be done. From Proposition 9 (with “min” and “max” appropriately interchanged) we have that:

$$f^{\hat{x}}(x) = \min_{i \in \mathcal{I}, j \in \mathcal{J}} 2 \frac{(C_i^{\hat{x}} - B_j^{\hat{x}})x + (h_i^{\hat{x}} - g_j^{\hat{x}})}{(C_i^{\hat{x}} + B_j^{\hat{x}})x + (h_i^{\hat{x}} + g_j^{\hat{x}})}. \quad (40)$$

Furthermore, from (34) and (35) we have that:

$$\tilde{f}^{\hat{x}}(x) = \min_{i \in \mathcal{I}, j \in \mathcal{J}} \tilde{f}_{i,j}^{\hat{x}}(x), \quad (41)$$

Table 2 fabrication-adaptive Optimization Algorithm for Bandgap Problems.

Algorithm FA-B for Bandgap Problems	
Step 1.	Start with initial guess $\hat{x} := x^0$ and tolerance ϵ_{tol}
Step 2a.	Construct the linear operators for (37) based on \hat{x} , for each $t \in \{1, \dots, n_k\}$: $\mathcal{A}_{\ell,t}^{\hat{x}}(x) := A_{\ell,t,0}^{\hat{x}} + \sum_{i=1}^{n_x} A_{\ell,t,i}^{\hat{x}} x_i$ $\mathcal{A}_{u,t}^{\hat{x}}(x) := A_{u,t,0}^{\hat{x}} + \sum_{i=1}^{n_x} A_{u,t,i}^{\hat{x}} x_i$ $M_{\ell,t}^{\hat{x}} \text{ and } M_{u,t}^{\hat{x}}$
Step 2b.	Construct the data for (38) based on \hat{x} and the linear operators from Step 2a: $B^{\hat{x}}, g^{\hat{x}}, C^{\hat{x}}, \text{ and } h^{\hat{x}}$
Step 3.	For each $(i, j) \in \mathcal{I} \times \mathcal{J}$, do: Compute the function value $\tilde{f}_{i,j}(\hat{x})$ of (42) via (29) Compute first-order information $\nabla \tilde{f}_{i,j}(\cdot)$ at \hat{x} via (30)
Step 4.	Form the linear optimization problem (44)
Step 5.	Solve (44) for an optimal solution x^*
Step 6.	If $\ x^* - \hat{x}\ \leq \epsilon_{\text{tol}}$, stop. Else update $\hat{x} \leftarrow x^*$ and go to Step 2.

where for each $(i, j) \in \mathcal{I} \times \mathcal{J}$ we have:

$$\begin{aligned} \tilde{f}_{ij}^{\hat{x}}(x) := \min_y & 2 \frac{(C_i^{\hat{x}} - B_j^{\hat{x}})y + (h_i^{\hat{x}} - g_j^{\hat{x}})}{(C_i^{\hat{x}} + B_j^{\hat{x}})y + (h_i^{\hat{x}} + g_j^{\hat{x}})} \\ \text{s.t.} & \|y - x\| \leq \delta \\ & y \in S. \end{aligned} \quad (42)$$

It also follows that $\tilde{f}_{ij}^{\hat{x}}(x)$ and $\nabla \tilde{f}_{ij}^{\hat{x}}(x)$ are computable via the convex optimization problems described in Propositions 7 and 8, respectively, and that Algorithm FA of Table 1 can be adapted (taking into account that the roles of min and max are switched and that the linear fractional pieces are indexed by pairs (i, j)) to solve the fabrication-adaptive optimization problem. The format for (28) becomes:

$$\begin{aligned} \max_{x \in S} \tilde{f}^{\hat{x}}(x) &= \max_{x,t} t \\ \text{s.t.} & \tilde{f}_{i,j}^{\hat{x}}(x) \geq t, \quad \text{for all } (i, j) \in \mathcal{I} \times \mathcal{J} \\ & x \in S, \end{aligned} \quad (43)$$

and the linearization of (43) at \hat{x} then is:

$$\begin{aligned} \max_{x,t} & t \\ \text{s.t.} & \tilde{f}_{i,j}^{\hat{x}}(\hat{x}) + (\nabla \tilde{f}_{i,j}^{\hat{x}}(\hat{x}))^T (x - \hat{x}) \geq t, \quad \text{for all } (i, j) \in \mathcal{I} \times \mathcal{J} \\ & x \in S. \end{aligned} \quad (44)$$

Table 2 presents the version of Algorithm FA, which we call Algorithm FA-B, for solving bandgap problems.

4. Computational Results for Fabrication-Adaptive Optimization

We first test the intended effectiveness of Algorithm FA (Table 1) on random problems. These results are presented in Section 4.1. We then apply Algorithm FA-B to a variety of bandgap

problems that arise in photonic crystal design, which was the problem class that engendered this line of research. We show via several examples how the solutions produced by Algorithm FA-B succeed in producing improved fabricable design solutions compared to solutions based on the optimal solution of the original design optimization problem. These results are presented in Section 4.2.

4.1. Computation on Random Piecewise Linear Fractional Problems

We tested Algorithm FA on randomly generated instances of the specially structured piecewise linear fractional optimization problem (32) presented in Section 2.5. All problems were generated using $n = 50$, $n_{\mathcal{I}} = 20$, and $n_{\mathcal{J}} = 30$, and S set to a unit hypercube of the form $S := \{x \in \mathbb{R}^n : 1.0 \leq x_i \leq 2.0, i = 1, \dots, n\}$. All of the components of a^i, c^j, g_i, h_j were chosen randomly from the uniform distribution $\mathcal{U}[0, 1]$, for $i = 1, \dots, n_{\mathcal{I}}, j = 1, \dots, n_{\mathcal{J}}$. The choice of S , the range of the data and the size of the generated problems are in close agreement with problems arising in photonic crystal design problems to be discussed in Section 4.2.

Given a randomly generated instance of (32), let us denote the optimal solution of the original optimization problem (32) as:

$$x_O^* := \arg \min_{x \in S} f(x). \quad (45)$$

To construct the fabrication-adaptive optimization problem, we used the norm $\|\cdot\| := \|\cdot\|_1$ and set $\delta = 5.0$, and note that this choice allows for changing up to 10% (5/50) of the components x_i of x by one unit, which is the full range of x_i by definition of S . Let x_{FA}^* denote the computed solution of the fabrication-adaptive optimization problem using Algorithm FA.

Note that x_O^* is the optimal solution of (32) which is solvable as a linear optimization problem. In contrast, x_{FA}^* is not necessarily the (global) optimal solution of FA optimization problem (28) and is computed using Algorithm FA (Table 1). Here and in what follows we used the Gurobi Optimizer (Gurobi Optimization 2013) to solve all linear optimization problems.

We generated 20 random instances of (32). Since the results of all 20 instances lead to the same conclusion, we only discuss detailed results from a particular one. For this problem instance the optimal objective function value of the original problem is $f(x_O^*) = 0.129$, whereas the value of the original objective function evaluated at the fabrication-adaptive solution is $f(x_{FA}^*) = 0.135$, which is inferior (larger) to that of the optimal value as expected. We tested the adaptivity of x_O^* and x_{FA}^* as follows. For these two solutions under consideration, and a given value of $\sigma \in [0, \delta]$, we compute the most conservative objective function value $f(y)$ among all solutions y for which $\|y - \hat{x}\| \leq \sigma$ and $y \in S$. That is, we compute:

$$\begin{aligned} \text{ZAD}^{\hat{x}}(\sigma) := \max_{y} \quad & f(y) \\ \text{s.t.} \quad & \|y - \hat{x}\| \leq \sigma \\ & y \in S, \end{aligned} \quad (46)$$

for $\hat{x} = x_O^*$ and $\hat{x} = x_{FA}^*$. One can interpret (46) as computing the worst solution y whose distance from \hat{x} is at most σ . In the absence of an intelligent method for adapting a solution \hat{x} , (46) essentially assumes the solution \hat{x} will be adapted to a nearby solution y in an *adversarial* manner (hence the choice of notation “ZAD” in (46)). The values of $\text{ZAD}^{\hat{x}}(\sigma)$ were computed using Steps 2 – 4 of Algorithm FA in Table 1. Plots of $\text{ZAD}^{x_O^*}(\sigma)$ and $\text{ZAD}^{x_{FA}^*}(\sigma)$ for $\sigma \in [0, \delta]$ are shown in Figure 2(a). For small values of σ , the range of adversarial solutions is small, and hence the superior original objective function value of x_O^* yields $\text{ZAD}^{x_O^*}(\sigma) < \text{ZAD}^{x_{FA}^*}(\sigma)$. However, as the values of σ increases, the superior adaptability of the solution x_{FA}^* is revealed. When the range of adversarial solutions is larger, $\text{ZAD}^{x_O^*}(\sigma) > \text{ZAD}^{x_{FA}^*}(\sigma)$, showing that nearby adversarial solutions

of x_{FA}^* are superior to those of x_O^* . These plots reveal that the solution x_{FA}^* is indeed effectively more adaptive, with the advantage growing as the allowable range of nearby solutions grows. We also repeated this computational exercise using $\delta = 10.0$. The resulting plots of $ZAD^{x_O^*}(\sigma)$ and $ZAD^{x_{FA}^*}(\sigma)$ for the case of $\delta = 10.0$ are shown in Figure 2(b). Notice that the results for the case $\delta = 10.0$ further reinforce the above observations.

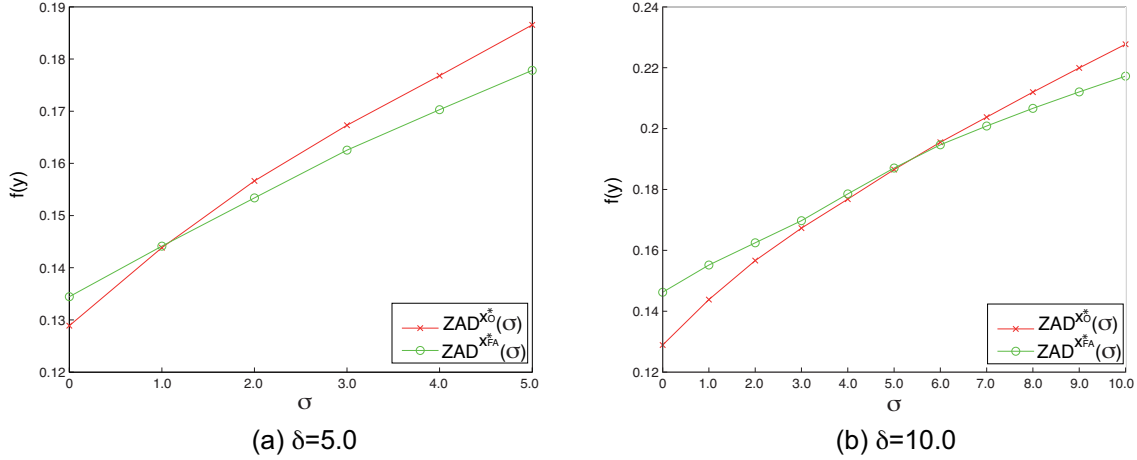


Figure 2 Adaptivity of x_O^* and x_{FA}^* to nearby *adversarial* solutions, as defined in (46).

Of the 20 randomly generated instances of (32), all exhibited similar effectiveness of the adaptivity of x_{FA}^* in terms of $ZAD^{x_O^*}(\sigma)$ and $ZAD^{x_{FA}^*}(\sigma)$.

4.2. Computational Experience on Bandgap Problems in Photonic Crystal Design

In this section we present results from applying the fabrication-adaptive optimization model to bandgap problems in photonic crystal design, which was the originator of our need to pursue this line of research. As briefly reviewed in Section 3, the goal is to optimize the bandgap between two consecutive eigenvalues, where the bandgap is the largest gap that separates the two eigenvalues over all values of k in the governing index set \mathcal{Q} . We seek to solve fabrication-adaptive models (43) using Algorithm FA-B (Table 2). There are many different types of bandgap optimization problems that one can construct as well as different schemes themselves for constructing bandgap optimization problems in photonic crystal design. For example, one arrives at different bandgap optimization problems depending on which eigenvalue gap one seeks to optimize (the m^{th} bandgap, defined as the relative gap between the m^{th} and the $(m+1)^{\text{st}}$ eigenvalues for $m = 1, \dots, N-1$), the choice of polarization (TE or TM or complete (TEM) polarization), and the lattice structure of the photonic crystal (typically a square lattice or a triangular lattice). Different combinations of these choices lead to different bandgap optimization problems with different optimal solutions. Among the numerous topological varieties in the optimal structures derived from different bandgap problems, one often encounters solutions that are either not fabricable or pose onerous fabrication challenges due to thin connectors, small features, rough edges, isolated structures, and other related solution configurations.

Among the roughly 60+ bandgap problems that we have solved, the original optimal solutions of at least 15 are not fabricable without post-processing modification. Furthermore, most of the non-fabricable solutions are for optimization problems for complete (TEM) bandgaps or other multiple-bandgap problems (Men 2011, Men et al. 2011). We applied the fabrication adaptive

optimization paradigm and algorithms to most of these problems. Herein we report on some of our computational experience to address questions such as: (i) how sensitive are solutions of the original problem to fabrication adaptivity modifications?, (ii) how good are the solutions computed when solving the fabrication-adaptive optimization problem?, and (iii) how do fabrication adaptive solutions compare to solutions of the original optimization problem?

For a given problem instance, let x_O^* be the optimal solution of the original bandgap problem (37) (or (38)) and let x_{FA}^* be the computed solution of the fabrication-adaptive optimization problem using Algorithm FA-B. In the case when x_O^* and/or x_{FA}^* are not fabricable, we applied manual changes of these solutions to produce fabricable solutions y_{FA} and/or y_O by using our own problem-domain common sense to modify pixel values to create more fabricable designs. The manual changes we employed are of the ordinary variety such as removing thin rods, removing small features, smoothing boundaries of materials, and straightening inner edges of material boundaries. All of these modifications can be easily accomplished with standard image processing filters.

As in Section 4.1, let x_O^* be the optimal solution of the original bandgap problem (37) (or (38)). An example of the poor performance of x_O^* after modification for fabrication arises in solving for the 2nd TE bandgap in the square lattice, as shown in Figure 3. Figure 3(a) shows the design x_O^* which has a bandgap of 65.6%, but which contains very thin rods that are challenging to fabricate. One can remove the thin rods by modifying 3% of the pixels, yielding the design y_O shown in part (b) of Figure 3. However, this small modification of the fabricable solution y_O drastically reduces the bandgap, from 65.6% down to 20.3%. Figure 3(c) shows the computed solution x_{FA}^* of the fabrication-adaptive optimization problem using Algorithm FA-B, for the value of $\delta = 3\%$. Not only is the bandgap for x_{FA}^* much higher (49.6%) than that of y_O , but it actually is fabricable as is. This is very fortunate, but perhaps “accidental”, as it is more typical that the solution x_{FA}^* would need to be modified to a nearby solution as we will see below. The main point of this example is to show how unadaptable the solution x_O^* can be to modification that will make it fabricable without unduly reducing the size of the bandgap.

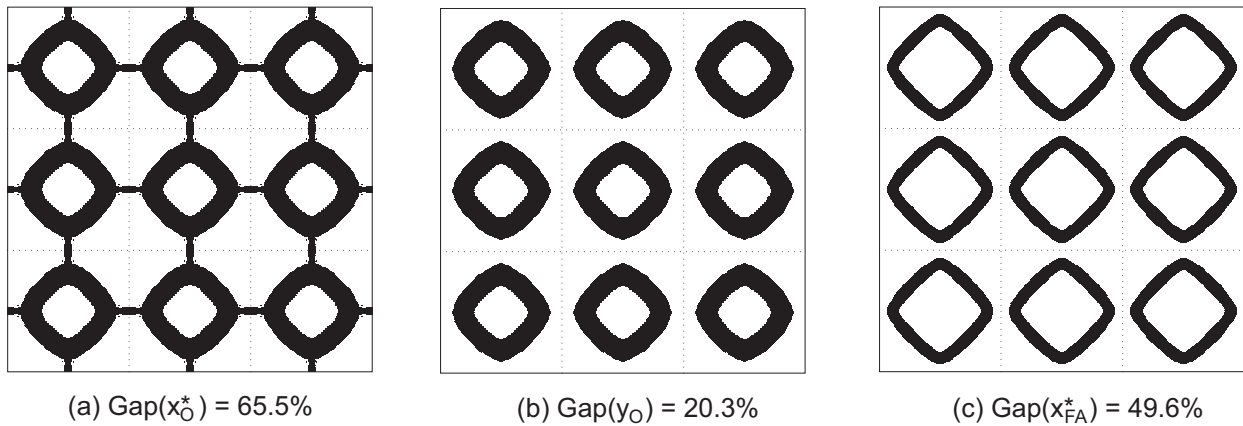


Figure 3 Solutions to the 2nd TE bandgap problem in the square lattice. (a) is the original optimal design x_O^* , with $\text{Gap}(x_O^*) = 65.5\%$; (b) is the solution y_O which is a manual modification of x_O^* , with $\text{Gap}(y_O) = 20.3\%$, and 3% of pixels being modified; (c) is the computed solution x_{FA}^* of using Algorithm FA-B, with $\text{Gap}(x_{FA}^*) = 49.6\%$, using $\delta = 3\%$.

An example of the quality of solutions computed using Algorithm FA-B is shown in Figure 4, which shows solutions to the complete (TEM) bandgap problem involving the 1st TE bandgap and the 2nd TM bandgap, in the triangular lattice. For this bandgap problem the bandgap for the original (non-fabricable) solution x_O^* (Figure 4(a)) is 33.3%. Figure 4(b) shows the computed

solution x_{FA}^* of the fabrication-adaptive optimization problem using Algorithm FA-B, for the value of $\delta = 5\%$. Figure 4(c) shows the manually modified solution y_{FA} of x_{FA}^* , with about 4% of pixels being modified. y_{FA} is significantly more fabricable than x_O^* , yet its bandgap value 31.9% is only modestly decreased from that of the original (non-fabricable) solution.

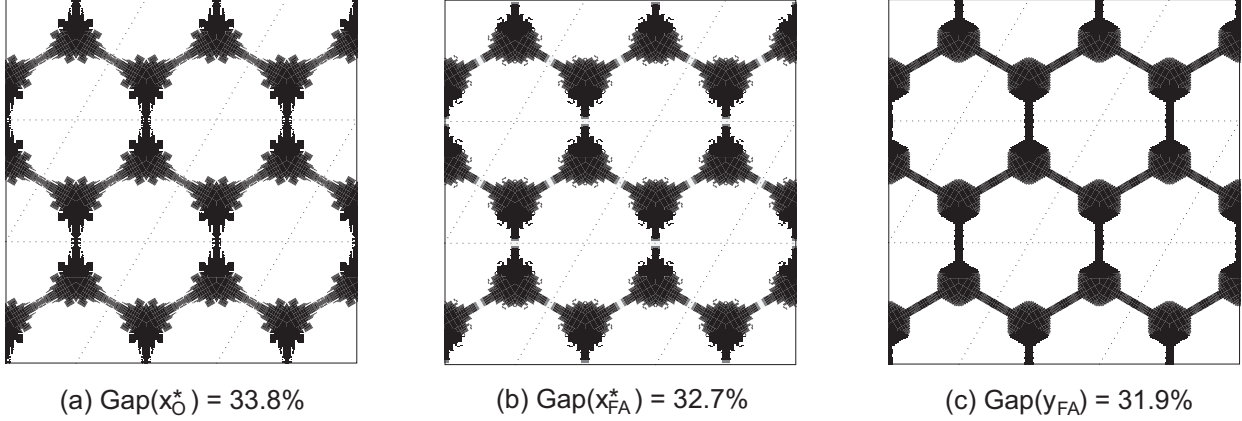


Figure 4 Solutions to the complete (TEM) bandgap problem involving the 1st TE bandgap and the 2nd TM bandgap, in the triangular lattice. (a) is the original optimal design x_O^* , with $\text{Gap}(x_O^*) = 33.8\%$; (b) is the computed solution x_{FA}^* using Algorithm FA-B, with $\text{Gap}(x_{FA}^*) = 32.7\%$, using $\delta = 5\%$; (c) is the solution y_{FA} which is a manual modification of x_{FA}^* , with $\text{Gap}(y_{FA}) = 31.9\%$, and 4% modification.

Our last two examples illustrate the comparative value of the fabrication-adaptive optimization approach. First we solve for the 5th TE bandgap in the triangular lattice, as shown in Figure 5. By simply eliminating the small features of the original optimal solution x_O^* shown in Figure 5(a) (which comprise 5% of the pixels), the bandgap of the manually modified solution y_O is sharply decreases from 43.9% to 28.8%. However, the fabrication-adaptive computed solution using Algorithm FA-B (using the same modification allowance $\delta = 5\%$ of pixels) yields the solution x_{FA}^* (shown in Figure 5(c)). The manual modification of this solution is y_{FA} , and is shown in Figure 5(d). The modified solution y_{FA} is designed so that the inner edges of the triangular structures in x_{FA}^* are straight, in order to make the resulting solution more fabricable. The resulting bandgap of the modified solution y_{FA} is 32.9%, which is better than that of the fabricable solution y_O based on the original optimal solution.

A similar situation occurs to solutions of the 4th TE bandgap in the square lattice. Figure 6(a) and Figure 6(b) show the original optimal solution and its manual modification to a fabricable solution by removing the thin rods, which reduces the original bandgap from 64.3% to 28.8%. In contrast, the computed solution x_{FA}^* shown in Figure 6(c) is truly more adaptive to modification for fabrication. Figure 6(d) shows the manually modified solution y_{FA} of x_{FA}^* , which was done by straightening the inner sides of the square structures. In the manual modifications of both solutions x_O^* and x_{FA}^* , the fraction of pixels modified was very small, both are roughly 1.2%. However, in the case of the original solution, the bandgap was significantly reduced (from 64.3% to 28.8%), while in the case of the fabrication-adaptive solution the bandgap reduction was minor (from 45.8% to 43.7%).

These examples show that while manual modification of solutions might appear to be minor, the negative effect on the bandgap can be very significant at solutions to the original problem, but (as intended) are less significant at computed solutions to the fabrication-adaptive optimization problem.

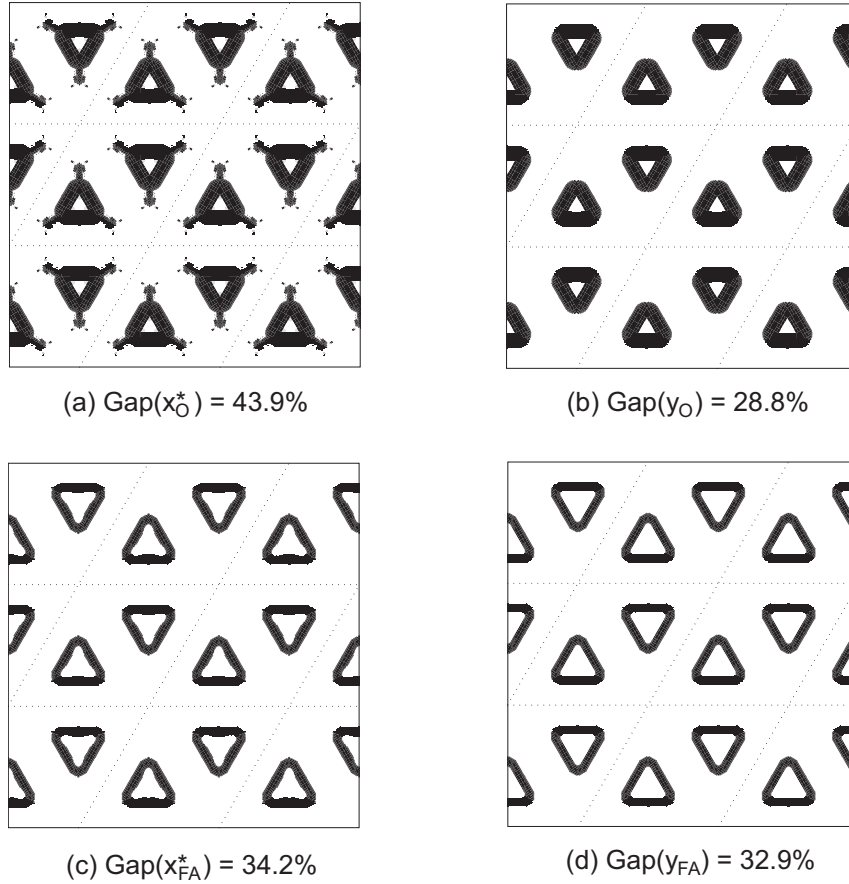


Figure 5 Designs with 5th TE eigenbandgap in a triangular lattice. (a) original optimal design x_O^* , with $\text{Gap}(x_O^*) = 43.9\%$; (b) manually modified design y_O based on the original design, with $\text{Gap}(y_O) = 28.8\%$, and 5% modifications; (c) Fabrication-Adaptive optimal design x_{FA}^* , with $\text{Gap}(x_{FA}^*) = 34.2\%$, and $\delta_{FA} = 5\%$; (d) manually modified design y_{FA} based on the FA optimal design, with $\text{Gap}(y_{FA}) = 32.9\%$, and 0.8% modification.

5. Conclusions

We have introduced the *fabrication-adaptive* optimization modeling paradigm (2)-(3), which stems from the *robust regularization* operation on functions (Lewis 2002). The FA modeling paradigm does not necessarily yield a convex optimization model even when the original optimization problem is convex. Hence, we examined a variety of special structures on functions, feasible regions, and norms, for which computation is tractable, and we developed an algorithmic scheme for solving certain FA optimization problems that arise from piecewise linear fractional optimization. We first tested the FA paradigm and algorithm on randomly generated problems to show some general behavior of solutions. We next applied our methodology to bandgap optimization problems in photonic crystal design, which were the originating class of problems that engendered this line of research. These bandgap problems were originally modeled using SDP formulations of iteration-specific approximation problems. To apply the FA framework, we developed piecewise linear approximations of the semidefinite inclusions, which worked surprisingly well and enabled replacing SDP inclusions with linear inequalities that yielded linear optimization problems. We used the FA model and algorithm to compute significantly improved fabricable designs of a variety of bandgap optimization problems in photonic crystal design.

As mentioned above, the success of piecewise linear approximations of the semidefinite inclusions in bandgap optimization models is counter to traditional notions that such approximations are

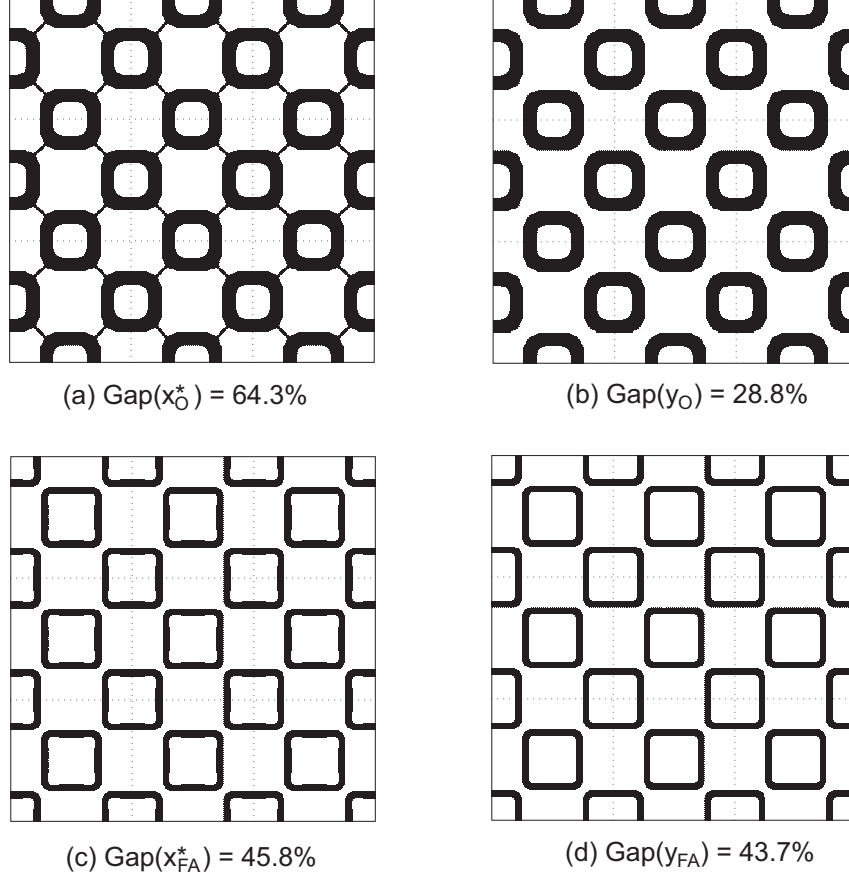


Figure 6 Solutions to the 4th TE bandgap in the square lattice. (a) is the original optimal design x_O^* , with $\text{Gap}(x_O^*) = 64.3\%$; (b) is the solution y_O which is a manual modification of x_O^* , with $\text{Gap}(y_O) = 28.8\%$, and 1.2% of pixels being modified; (c) is the computed solution x_{FA}^* using Algorithm FA-B, with $\text{Gap}(x_{FA}^*) = 45.8\%$, using $\delta = 5\%$; (d) is the solution y_{FA} which is a manual modification of x_{FA}^* , with $\text{Gap}(y_{FA}) = 43.7\%$, and also 1.2% of pixels being modified.

crude at best. It is unclear at this point whether the success of our simple LP/SDP approximation is due to the very specific structure of bandgap design problems and the resulting eigenvalue bound inclusions. Future research on our agenda includes other applications and extensions of fabrication-adaptive optimization, as well as exploration aimed at understanding the possible reach of success of the LP/SDP approximation method described in the Appendix B of this paper.

Appendix A: Relation of Fabrication-Adaptive Optimization Model to Robust Optimization

In the special case when $S = \mathbb{R}^n$, one can re-formulate the fabrication-adaptive optimization problem (3) as a particular instance of a robust optimization problem (Ben-Tal et al. 2009), at least conceptually. Let us see how this can be done. We first use the change of variable $d := y - x$ and note that when $S = \mathbb{R}^n$ we can re-write (2) as:

$$\begin{aligned} \tilde{f}(x) = \max_d \quad & f(x + d) \\ \text{s.t.} \quad & \|d\| \leq \delta \\ & d \in \mathbb{R}^n. \end{aligned} \tag{47}$$

Considering d as the “data” we can define the function $\hat{f}_d(x) := f(x + d)$ for $x, d \in \mathbb{R}^n$, where the “data” d parametrically defines the function $\hat{f}_d(\cdot)$. Then notice that the level set condition “ $\tilde{f}(x) \leq t$ ” obeys:

$$\tilde{f}(x) \leq t \quad \Leftrightarrow \quad \hat{f}_d(x) \leq t \text{ for all } d \in B(0, \delta), \tag{48}$$

where $B(c, r)$ denotes the ball centered at c with radius r . Therefore, we can write the fabrication-adaptive optimization problem (3) as:

$$\begin{aligned} \tilde{z}^* &= \min_{x,t} t \\ \text{s.t. } & \hat{f}_d(x) \leq t \text{ for all } d \in B(0, \delta) . \end{aligned} \quad (49)$$

Observe that (49) corresponds exactly to a robust optimization model with uncertain “data” d used as the “data” parameter of the function $\hat{f}_d(x) := f(x+d)$, and with the uncertainty set $\mathcal{U} := B(0, \delta)$. In the language of robust optimization, the constraints of (49) immunize the inequality “ $f(x) \leq t$ ” over all possible values of the data d in the uncertainty set $\mathcal{U} := B(0, \delta)$. If $f(\cdot)$ is a convex function, then $\hat{f}_d(\cdot)$ is convex for any d , whereby $\tilde{f}(x) = \max_{d \in B(0, \delta)} \hat{f}_d(x)$ is also convex as it is the pointwise maximum of convex functions. (This also provides an alternate proof that the fabrication-adaptive optimization problem (3) is a convex optimization problem when $S = \mathbb{R}^n$.)

When $S \neq \mathbb{R}^n$, we show that the above analysis breaks down. In the general case of $S \subset \mathbb{R}^n$ the fabrication-adaptive optimization problem (3) can be re-written as:

$$\begin{aligned} \tilde{z}^* &= \min_{x,t} t \\ \text{s.t. } & f_d(x) \leq t \text{ for all } d \in B(0, \delta) \cap (S - \{x\}) \\ & x \in S . \end{aligned} \quad (50)$$

Now notice in (50) that the corresponding “uncertainty set” is now $\mathcal{U} = \mathcal{U}(x) := B(0, \delta) \cap (S - \{x\})$ which depends on the decision variable x . The lack of independence of the uncertainty set $\mathcal{U} = \mathcal{U}(x)$ from the value of the variable x leads to the potential for the problem (50) to be non-convex even when $f(\cdot)$ is convex and the feasible region S is convex. It was already shown in Section 1.1 that one can easily construct such an instance where the resulting fabrication-adaptive optimization problem is not convex and is not even quasi-convex.

Appendix B: Relaxation and Reformulation of the bandgap Optimization Problem

B.1. Approximation of the Eigenvalue Bounds using Linear Inequalities

While we would like to apply the fabrication-adaptive methodology to the bandgap optimization problem, the third example in Section 2.1 illustrates the challenges in doing so. The objective function of the bandgap optimization problem (37) is at least as complicated as the largest eigenvalue function (7), whose fabrication-adaptive counterpart is not generally tractable to compute as discussed in Section 2.1. However, Example 2.5 shows that if $f(\cdot)$ is a special piecewise linear fractional function, then its fabrication-adaptive counterpart $\tilde{f}(\cdot)$ is tractable to compute. We therefore propose to replace the eigenvalue bounds in (37), which are modeled with semidefinite inclusions, with piecewise linear approximations that are modeled with linear inequalities, thereby replacing (37) with a linear fractional optimization problem of the form (38). We carry out this step as follows.

The matrix data in (37) are constructed as “reduced” stiffness and mass matrices based on the current iterate $\hat{x} \in S$, and are given by (see Men et al. (2010)):

$$\begin{aligned} \mathcal{A}_{\ell,t}^{\hat{x}}(x) &:= A_{\ell,t,0}^{\hat{x}} + \sum_{i=1}^{n_x} A_{\ell,t,i}^{\hat{x}} x_i := \Phi_{\ell}^{\hat{x}}(k_t)^* \mathbf{A}_0(k_t) \Phi_{\ell}^{\hat{x}}(k_t) + \sum_{i=1}^{n_x} (\Phi_{\ell}^{\hat{x}}(k_t)^* \mathbf{A}_i(k_t) \Phi_{\ell}^{\hat{x}}(k_t)) x_i, \\ M_{\ell,t}^{\hat{x}} &:= \Phi_{\ell}^{\hat{x}}(k_t)^* \mathbf{M} \Phi_{\ell}^{\hat{x}}(k_t), \\ \mathcal{A}_{u,t}^{\hat{x}}(x) &:= A_{u,t,0}^{\hat{x}} + \sum_{i=1}^{n_x} A_{u,t,i}^{\hat{x}} x_i := \Phi_u^{\hat{x}}(k_t)^* \mathbf{A}_0(k_t) \Phi_u^{\hat{x}}(k_t) + \sum_{i=1}^{n_x} (\Phi_u^{\hat{x}}(k_t)^* \mathbf{A}_i(k_t) \Phi_u^{\hat{x}}(k_t)) x_i, \\ M_{u,t}^{\hat{x}} &:= \Phi_u^{\hat{x}}(k_t)^* \mathbf{M} \Phi_u^{\hat{x}}(k_t), \end{aligned} \quad (51)$$

for $t = 1, \dots, n_k$. The subspace matrices $\Phi_\ell^{\hat{x}}(k_t)$ and $\Phi_u^{\hat{x}}(k_t)$ consist columnwise of the “important” eigenfunctions,

$$\Phi_\ell^{\hat{x}}(k_t) = [u_a(k_t, \hat{x}), \dots, u_m(k_t, \hat{x})], \quad \Phi_u^{\hat{x}}(k_t) = [u_{m+1}(k_t, \hat{x}), \dots, u_b(k_t, \hat{x})]. \quad (52)$$

The following result is obtained as a consequence of the derivation of these matrices from the Finite Element Method and from the fact that the basis sets $\Phi_\ell^{\hat{x}}(k_t)$, $\Phi_u^{\hat{x}}(k_t)$ are \mathbf{M} -orthogonal bases, see also Proposition 10.

PROPOSITION 13. *For all $x \in S$, the reduced stiffness and mass matrices (51) satisfy:*

1. $\mathcal{A}_{\ell,t}^{\hat{x}}(x) \succeq 0$, and $\mathcal{A}_{u,t}^{\hat{x}}(x) \succeq 0$ for $t = 1, \dots, n_k$,
2. $\mathcal{A}_{\ell,t}^{\hat{x}}(x) \succ 0$, and $\mathcal{A}_{u,t}^{\hat{x}}(x) \succ 0$ for $k_t \neq 0$, and
3. $M_{\ell,t}^{\hat{x}} \succ 0$, and $M_{u,t}^{\hat{x}} \succ 0$ for $t = 1, \dots, n_k$. \square

We next note that the semidefinite inclusions in (37) can be rewritten as:

$$\begin{aligned} b^T \mathcal{A}_{\ell,t}^{\hat{x}}(x) b &\leq \lambda_\ell b^T M_{\ell,t}^{\hat{x}} b, \quad t = 1, \dots, n_k, \quad \text{for all } b \in \mathbb{R}^{N_\ell}, \\ c^T \mathcal{A}_{u,t}^{\hat{x}}(x) c &\geq \lambda_u c^T M_{u,t}^{\hat{x}} c, \quad t = 1, \dots, n_k, \quad \text{for all } c \in \mathbb{R}^{N_u}. \end{aligned} \quad (53)$$

We will approximate the above conditions by judiciously generating a finite number of approximating vectors $b^{(1)}, \dots, b^{(N_B)} \in \mathbb{R}^{N_\ell}$ and $c^{(1)}, \dots, c^{(N_C)} \in \mathbb{R}^{N_u}$. (The method for choosing and updating these sets of vectors will be discussed in the next subsection.) The resulting linear inequalities in the variables x , λ_ℓ , and λ_u are:

$$\begin{aligned} (b^{(p)})^T A_{\ell,t,0}(b^{(p)}) + \sum_i^{n_\varepsilon} (b^{(p)})^T A_{\ell,t,i}(b^{(p)}) x_i &\leq \lambda_\ell (b^{(p)})^T M_{\ell,t}^{\hat{x}}(b^{(p)}), \quad t = 1, \dots, n_k, \quad p = 1, \dots, N_B, \\ (c^{(p)})^T A_{u,t,0}(c^{(p)}) + \sum_i^{n_\varepsilon} (c^{(p)})^T A_{u,t,i}(c^{(p)}) x_i &\geq \lambda_u (c^{(p)})^T M_{u,t}^{\hat{x}}(c^{(p)}), \quad t = 1, \dots, n_k, \quad p = 1, \dots, N_C. \end{aligned} \quad (54)$$

Because the mass matrices $M_{\ell,t}^{\hat{x}}$ and $M_{u,t}^{\hat{x}}$ are positive definite (Proposition 13), the coefficients in the right-hand-side of (54) are all positive. It follows that (54) can be reformatted by rescaling as the following two linear inequality systems:

$$B^{\hat{x}} x + g^{\hat{x}} \leq e \lambda_\ell, \quad C^{\hat{x}} x + h^{\hat{x}} \geq e \lambda_u, \quad (55)$$

where $B^{\hat{x}} \in \mathbb{R}^{(N_B n_k) \times n_x}$, and $C^{\hat{x}} \in \mathbb{R}^{(N_C n_k) \times n_x}$. It then follows from Proposition 13 that:

$$(B^{\hat{x}} x + g^{\hat{x}})_j > 0, \quad j = 1, \dots, N_B n_k =: \mathcal{N}_B \quad \text{and} \quad (C^{\hat{x}} x + h^{\hat{x}})_i > 0, \quad i = 1, \dots, N_C n_k =: \mathcal{N}_C, \quad (56)$$

for all $x \in S$.

Replacing the semidefinite inclusions in (37) with their linear inequality approximations (55), we obtain the following linear fractional approximation of (37):

$$\begin{aligned} P_{LFP}^{\hat{x}} : \max_{x, \lambda_\ell, \lambda_u} \quad & \frac{\lambda_u - \lambda_\ell}{\lambda_u + \lambda_\ell} \\ \text{s.t.} \quad & B^{\hat{x}} x + g^{\hat{x}} \leq e \lambda_\ell, \\ & C^{\hat{x}} x + h^{\hat{x}} \geq e \lambda_u, \\ & x_{\min} \leq x_i \leq x_{\max}, \quad i = 1, \dots, n_x \\ & \lambda_\ell \geq 0, \lambda_u \geq 0, \lambda_\ell + \lambda_u > 0. \end{aligned} \quad (57)$$

The superscript “ $(\cdot)^{\hat{x}}$ ” indicates that components of B , C , g , and h are functions of (and so depend on) \hat{x} . In order for the linear inequality formulation to be reasonably accurate, the optimal solution x^* of (57) should be close enough to the linearizing point \hat{x} , i.e., $\|x^* - \hat{x}\| \leq \epsilon$. Since the optimization

Table 3 Algorithm for solving bandgap problems using linear inequalities approximation of eigenvalue bounds.

Algorithm for Bandgap Optimization using Linear Inequalities Approximation	
Step 1.	Start with initial guess $\hat{x} := x^0$ and tolerance ϵ_{tol}
Step 2a.	Construct the matrices (51) for (37) based on \hat{x} , for each $t \in \{1, \dots, n_k\}$: $\mathcal{A}_{\ell,t}^{\hat{x}}(x) := A_{\ell,t,0}^{\hat{x}} + \sum_{i=1}^{n_x} A_{\ell,t,i}^{\hat{x}} x_i$ $\mathcal{A}_{u,t}^{\hat{x}}(x) := A_{u,t,0}^{\hat{x}} + \sum_{i=1}^{n_x} A_{u,t,i}^{\hat{x}} x_i$ $M_{\ell,t}^{\hat{x}} \text{ and } M_{u,t}^{\hat{x}}$
Step 2b.	Choose vectors b^1, \dots, b^{N_B} and c^1, \dots, c^{N_C} :
Step 2c.	Construct the data for (57) based on \hat{x} and the linear operators from Step 2a: $B^{\hat{x}}, g^{\hat{x}}, C^{\hat{x}}$, and $h^{\hat{x}}$
Step 3.	Form the linear fractional problem $P_{LFP}^{\hat{x}}$ in (57)
Step 4.	Solve $P_{LFP}^{\hat{x}}$ for an optimal solution $(x^*, \lambda_{\ell}^*, \lambda_u^*)$ <i>(Optional: augment $P_{LFP}^{\hat{x}}$ with Delayed Constraint Generation)</i>
Step 5.	If $\ x^* - \hat{x}\ \leq \epsilon_{\text{tol}}$, stop. Else update $\hat{x} \leftarrow x^*$ and go to Step 2 .

problem (57) is a linearly constrained linear fractional optimization problem, it can be converted to a linear program and efficiently solved by using standard linear optimization software. Table 3 presents the basic outline of the algorithm for solving bandgap optimization problems by the linear fractional optimization (57) instead of the semidefinite program (37). We note in Step 4 of the algorithm that one can augment the solution process for $P_{LFP}^{\hat{x}}$ with a standard delayed constraint generation procedure (Bertsimas and Tsitsiklis 1997). More detailed implementation of Step 2b is discussed in the next subsection.

B.2. Methodology for Constructing the Approximating Vectors

We describe our approach for constructing the approximating vectors $b^{(1)}, \dots, b^{(N_B)} \in \mathbb{R}^{N_{\ell}}$ and $c^{(1)}, \dots, c^{(N_C)} \in \mathbb{R}^{N_u}$. We focus on $b^{(1)}, \dots, b^{(N_B)} \in \mathbb{R}^{N_{\ell}}$, as the same approach is also used to construct the approximating vectors $c^{(1)}, \dots, c^{(N_C)} \in \mathbb{R}^{N_u}$. Note that N_{ℓ} (and N_u) is not large, typically $N_{\ell} \approx 3 - 7$, due to the subspace approximation. Ideally, we would want the approximating vectors to be distributed uniformly over the upper half of the Euclidean sphere: $\{b \in \mathbb{R}^{N_{\ell}} : \sqrt{b^T b} = 1, b_{N_{\ell}} \geq 0\}$, where we need only consider a half-sphere because $v^T M v = (-v)^T M (-v)$ for any $v \in \mathbb{R}^{N_{\ell}}$. For ease of construction, we choose to work with the upper half of the unit L_1 -sphere, also known as the upper boundary of the cross-polytope $\{b \in \mathbb{R}^{N_{\ell}} : \|b\|_1 = 1, b_{N_{\ell}} \geq 0\}$, whose $2^{(N_{\ell}-1)}$ facets are the unit $(N_{\ell} - 1)$ -simplices in their respective orthants. Given an integer dilation constant K , we first define:

$$\mathcal{K} := \left\{ k \in \mathbb{R}^{N_{\ell}} : \sum_{i=1}^{N_{\ell}} |k_i| = K, k_i \text{ integer} \right\}, \quad (58)$$

and then define the approximating vectors $b^{(1)}, \dots, b^{(N_B)} \in \mathbb{R}^{N_{\ell}}$ to be the elements of the following set:

$$B_K := \left\{ b \in \mathbb{R}^{N_{\ell}} : b = (1/K)k \text{ for some } k \in \mathcal{K}, k_{N_{\ell}} \geq 0 \right\}.$$

The resulting approximating vectors are distributed uniformly on the surface of the half cross-polytope. This is illustrated in Figure 7 for $N_{\ell} = 2$. Note that the number of vectors in B_K grows as

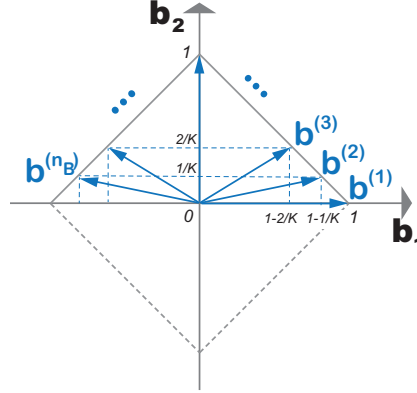


Figure 7 The vectors chosen to construct the approximating linear inequalities are distributed uniformly on the surface of a half cross-polytope arising from the L_1 norm.

$O(K^{N_\ell-1})$. Increasing K will render the piecewise linear approximation model more accurate albeit at higher computational cost. In addition and if necessary, we expand the set of approximating vectors at each iteration using delayed constraint generation: once the linear fractional optimization problem (57) is solved, we check the semidefinite inclusions in (37) for any eigenvectors violating the constraints and add them to the set of approximating vectors to generate additional linear inequality cuts which are then added to (57). Note that checking the semidefinite inclusions in (37) is inexpensive due to the reduced size of the system.

B.3. Quality of Linear Inequalities Approximation

To verify the quality of the approximation of the semidefinite inclusions by using the above approach, we focus on the effect of the tunable parameter K (defined in equation (58)) and the resulting number of linear inequalities. We first note that when K is large, more vectors (larger N_B and N_C) are generated to presumably approximate semidefinite inclusions more accurately, yielding a linear fractional optimization problem (57) that better approximates the semidefinite problem (37). As a result, the resulting linear optimization problem will contain a larger number of linear inequalities and thus require more computation time. On the other hand, a smaller value of K will reduce the number of linear inequality constraints, but result in a less accurate approximation of (37). The quality of the linear inequalities approximation may be empirically measured in terms of the number of outer iterations of the algorithm of Table 3 and the number of “successful” solutions, where a solution is deemed successful if it opens up a bandgap more than 10%.

We conduct an empirical test in order to determine a good value of K . In particular, we make 10 runs of the algorithm of Table 3 using 10 randomly chosen starting point configurations for a variety of types of bandgap problems and report the results in Table 4. In this table, the headings in the right side columns of the form $\Delta_{1,2}^{TE}$ refer to bandgap optimization of the bandgap between the 2nd and 1st eigenvalues in TE polarization, etc. Table 4 shows average outer iterations, and number of successful runs, for various bandgap optimization problems by using the algorithm of Table 3, with a large value of K ($K = 5$, resulting in $N_B, N_C \sim 500$) and a small value of K ($K = 3$, resulting in $N_B, N_C \sim 10$) combined with delayed constraint generation (DCG). The results of the SDP approach (presented in Men et al. (2010)) are shown in the table as a benchmark for comparison. We observe that using a small value of $K = 3$ combined with delayed constraint generation appears to strike a good compromise between system size (and computation time) and the success rate.

Acknowledgments

This work is supported by AFOSR Grant No. FA9550-11-1-0141, the Singapore-MIT Alliance, the MIT-Chile-Pontificia Universidad Catlica de Chile Seed Fund, and LaCaixa Fellowship.

Table 4 Average number of outer iterations and the total number of successful runs (out of 10 runs) for bandgap optimization using the semidefinite program (SDP) formulation and the linear fractional program (LFP) formulation. $\Delta\lambda_{m,m+1}$ indicates the optimized bandgap is between the m^{th} and the $(m+1)^{\text{st}}$ eigenvalues. DCG denotes delayed constraint generation.

Bandgap	$\Delta\lambda_{1,2}^{TE}$	$\Delta\lambda_{2,3}^{TE}$	$\Delta\lambda_{8,9}^{TE}$	$\Delta\lambda_{9,10}^{TE}$
SDP	9.0/7	9.0/6	14.2/2	23.5/1
LFP ($K = 5$)	17.0/9	9.1/8	43.5/3	40.5/3
LFP ($K = 3$)	20.0/6	12.6/6	37.1/1	26.1/2
LFP ($K = 3$) with DCG	14.0/8	15.8/6	27.7/3	24.1/4

(a) TE polarization

Bandgap	$\Delta\lambda_{1,2}^{TM}$	$\Delta\lambda_{2,3}^{TM}$	$\Delta\lambda_{8,9}^{TM}$	$\Delta\lambda_{9,10}^{TM}$
SDP	3.4/10	4.1/8	10.9/3	22.5/2
LFP ($K = 5$)	5.1/10	10.2/7	31.2/3	36.1/4
LFP ($K = 3$)	5.2/10	6.3/8	20.5/2	34.2/2
LFP ($K = 3$) with DCG	5.2/10	6.9/7	23.2/2	27.6/2

(b) TM polarization

References

- Avriel, M. 1976. *Nonlinear Optimization: Analysis and Methods*. Prentice-Hall.
- Ben-Tal, A., L. El Ghaoui, A. Nemirovski. 2009. *Robust optimization*. Princeton University Press.
- Ben-tal, A., A. Nemirovski. 2002. On tractable approximations of uncertain linear matrix inequalities affected by interval uncertainty. *SIAM Journal on Optimization* **12** 811–833.
- Bertsimas, D., J. Tsitsiklis. 1997. *Introduction to Linear Optimization*. Athena Scientific.
- Bertsimas, Dimitris, David B Brown, Constantine Caramanis. 2011. Theory and applications of robust optimization. *SIAM review* **53**(3) 464–501.
- Best, M. 2010. *Portfolio Optimization*. CRC Press.
- Borwein, J., A. Lewis. 2006. *Convex Analysis and Nonlinear Optimization*. Springer.
- Boyd, S., L. Vandenberghe. 2004. *Convex Optimization*. Cambridge University Press.
- Charnes, A., W. W. Cooper. 1962. Programming with linear functionals. *Naval Research Logistics Quarterly* **9**.
- Cox, S. J., D. C. Dobson. 2000. Band structure optimization of two-dimensional photonic crystals in H-polarization. *Journal of Computational Physics* **158**(2) 214–224.
- Craven, B.D., B. Mond. 1973. The dual of a fractional linear program. *Journal of Mathematical Analysis and Applications* **42**(3) 507–512.
- Duffin, R.J. 1956. Infinite programs. H.W. Kuhn, A.W. Tucker, eds., *Linear Inequalities and Related Systems*. Princeton University Press, 157–170.
- Freund, R.M. 1985. Postoptimal analysis of a linear program under simultaneous changes in matrix coefficients. *Mathematical Programming Essays in Honor of George B. Dantzig Part I* 1–13.
- Gurobi Optimization, Inc. 2013. Gurobi optimizer reference manual. URL <http://www.gurobi.com>.
- Kao, C. Y., S. Osher, E. Yablonovitch. 2005. Maximizing band gaps in two-dimensional photonic crystals by using level set methods. *Applied Physics B: Lasers and Optics* **81**(2) 235–244.

- Lewis, A. 2002. Robust regularization. Technical report, Simon Fraser University.
- Lewis, A.S., C.H.J. Pang. 2009. Lipschitz behavior of the robust regularization. *SIAM Journal on Control and Optimization* **48**(5) 3080–3104.
- Luo, Zhi-Quan. 2003. Applications of convex optimization in signal processing and digital communication. *Mathematical programming* **97**(1-2) 177–207.
- Luo, Zhi-Quan, Jos F Sturm, Shuzhong Zhang. 2004. Multivariate nonnegative quadratic mappings. *SIAM Journal on Optimization* **14**(4) 1140–1162.
- Men, H. 2011. Optimal design of photonic crystals. Ph.D. thesis, National University of Singapore.
- Men, H., NC Nguyen, RM Freund, KM Lim, PA Parrilo, J. Peraire. 2011. Design of photonic crystals with multiple and combined band gaps. *Physical Review E* **83**(4) 046703.
- Men, H., NC Nguyen, RM Freund, PA Parrilo, J. Peraire. 2010. Bandgap optimization of two-dimensional photonic crystals using semidefinite programming and subspace methods. *Journal of Computational Physics* **229** 3706–3725.
- Nemirovski, A. 2012. private communication.
- Pinar, Mustafa Ç, Orhan Arıkan. 2004. On robust solutions to linear least squares problems affected by data uncertainty and implementation errors with application to stochastic signal modeling. *Linear algebra and its applications* **391** 223–243.
- Rockafellar, T. 1970. *Convex Analysis*. Princeton University Press.
- Sherali, Hanif D, Barbara MP Fraticelli. 2002. Enhancing rlt relaxations via a new class of semidefinite cuts. *Journal of Global Optimization* **22**(1-4) 233–261.
- Stinstra, Erwin, Dick Den Hertog. 2008. Robust optimization using computer experiments. *European Journal of Operational Research* **191**(3) 816–837.